# Reconstruction of the paleoenvironmental context of Holocene human behavior at the Fenghuangzui site in the Nanyang Basin, Middle Yangtze River, China

**Aipeng Guo**
Nanjing University of Information Science and Technology
**Longjiang Mao**
mlj1214@163.com

Nanjing University of Information Science and Technology
**Chenchen Li**
Nanjing University of Information Science and Technology
**Duowen Mo**
Peking University

**Research Article**

**Keywords:** Holocene, Middle Yangtze River, Environmental Evolution, Ancient City, Fenghuangzui Site

**Posted Date:** August 16th, 2024

**DOI:** https://doi.org/10.21203/rs.3.rs-4731265/v1



**Additional Declarations:** No competing interests reported.

**Version of Record:** A version of this preprint was published at npj heritage science on February 7th, 2025. See the published version at https://doi.org/10.1038/s40494-025-01631-z.

# Abstract

Prehistoric city sites, as pivotal aspects of early urban evolution, are intricately linked to regional environmental factors such as climate, geomorphology, and hydrology. However, due to the lack of reliable chronologies associated with these ancient sites, there is limited understanding of environmental factors in relation to prehistoric urban centers. This study focuses on the sedimentary records from the southern moat of the Fenghuangzui (FHZ) ancient city site, a representative site in the middle Yangtze River region, integrating a chronological framework and climate proxies such as elemental geochemistry. It reconstructs the evolution of the regional sedimentary environment and the hydrogeomorphology during the mid-late Holocene at the FHZ site, elucidating its interplay with human activities. Key findings include: (1) From 5.5 ~ 4.5 ka BP, elevated CIA, Rb/Sr, and Mn/Ti values indicate a warm and humid climate. The Qujialing culture unified the middle Yangtze River and expanded abroad, building prehistoric cities such as Shijiahe city. The FHZ city was built in the Nanyang Basin at this time to prevent the invasion of northern culture. (2) During 4.5 ~ 3.9 ka BP, decreased CIA and Rb/Sr values alongside rising Saf and Be values signify reduced weathering and a transition to cooler, drier conditions. A flood event of 4 ~ 3.9 ka BP caused the moat of the FHZ city to lose its defensive function. (3) During 3.9 ~ 2.7 ka BP, declining CIA and Rb/Sr values with slight increases in Saf and Be suggest ongoing dry and cool environmental conditions. The FHZ city was abandoned at the end of the Meishan culture. (4) Between 2.7 ~ 1.6 ka BP, rising CIA and Rb/Sr values indicate a return to warmer and more humid conditions. The FHZ site was built to expand the influence of Qujialing culture and protect the Shijiahe city. Taking into account the location of the water system and farming area, the south-facing direction was chosen. After a flood in 4.0 ~ 3.9 ka BP, the FHZ site lost their defense function and were invaded by Meishan culture. In general, our findings suggest that changes in regional hydrology in the context of climate change can trigger upheaval and even collapse of prehistoric societies.


# Introduction

Over the past approximately 20 ka, the global climate has undergone significant changes, marked by an overall warming trend from the Last Glacial Maximum (LGM) to the Holocene thermal maximum, followed by a general cooling trend [1–3]. During this interval, the dynamic interaction between climatic fluctuations and environmental changes influenced diverse civilizations and cultural landscapes [4, 5]. Recent studies frequently underscore the synchronicity between climatic events and significant cultural shifts. This encompasses the influence of natural elements, such as climatic fluctuations, precipitation patterns, and geomorphic evolution, on the settlement patterns, survival strategies, and sociocultural practices within human communities [6–9]. For example, the 4.2 ka BP event in the mid-late Holocene had varying degrees of impact on early civilizations [10]. During this period, the collapse of agrarian societies and large human migration events occurred in the Nile Valley and eastern China due to climatic droughts, among others [11, 12].The dwindling of river flooding spurred intensive agriculture in the Harappan civilization, yet the subsequent drying of monsoonal rivers led to a gradual migration towards the northern, more humid regions [13]. Thus, it is imperative to fully consider the roles of climatic and environmental factors to comprehensively understand the process of human civilization.

The generally warm climate of the Holocene provided favorable conditions for the development of agriculture during the Neolithic period [14, 15]. During this period, regions including the Nile Valley in Egypt [16], the Yellow River basin [17, 18], and the Yangtze River basin in China [19] experienced the Holocene Climate Optimum (HCO). The HCO fostered abundant water resources and fertile soils, facilitating the emergence of agriculture and prehistoric cities [20, 21]. The middle Yangtze River are influenced by the East Asian monsoon and have complex hydrological features, making them one of the origins of rice agriculture [22]. Between 6.5 and 5.3 ka BP, ancient cities such as Chengtoushan site, with structures like city walls, water fields, and water conservancy systems, appeared in the Dongting Lake Basin under favorable hydrological conditions. These settlements exhibited clear social hierarchical differentiation [19]. From 5.3 ~ 3.9 ka BP, many large and interconnected settlements emerged in the middle Yangtze River region, with about 20 ancient cities established and continuously used during this period [23]. However, precipitation alone could not meet the water demands of large city sites, necessitating the consideration of natural water systems in site selection and usage. Ring trenches, as important water management facilities, provided conveniences for flood control, drainage, transportation, military defense, and agricultural production [24]. Therefore, the establishment and use of ancient cities were closely linked to the geomorphology and hydrology of the regional environment. The climatic deterioration around 4.2 ka BP may have led to the decline of the culture in the middle Yangtze River, with many large settlements abandoned and gradually occupied by the northern Central Plains culture [25]. Previous studies have extensively explored the environmental evolution and human activities in the middle Yangtze River, focusing on large environmental datasets from sedimentary records in the Jianghan Plain [26] and Dongting Lake Plain [27], stalagmite records from Shanbao Cave in Shennongjia [28], and the distribution of Neolithic sites in relation to climatic change events [19, 25], as well as the reasons for the mass decline and migration of the settlement sites [29]. Despite the rich history of archaeological and paleoclimatic environmental studies in the middle Yangtze River, there remains a gap in studies that directly relate the regional environmental context to the development of ancient city sites.

The FHZ site, a Neolithic settlement, is located in the middle Yangtze River region at the southern edge of the Nanyang Basin. It is the largest and highest-grade central settlement site found so far in Nanyang Basin of Northwest Hubei. Recent research has shown that the construction of the FHZ city wall dates back to the Qujialing culture period, making it the highest known Qujialing culture site in terms of latitude. During the Shijiahe culture period, the FHZ city wall lost its defensive function. The moat was used only for irrigation, transforming the FHZ site from a city to a settlement centered on the moat. After the Meishan culture, the site was completely abandoned [30].The moat outside the city wall is connected to the Paizihe River, forming a water conservancy system. The remains of the city wall and the river of the ancient city show that the construction of the ancient city had a close connection with the natural environment. After a number of archaeological excavations, related scholars have studied the function, structure and identification of plant remains of the site [31, 32]. Although environmental factors evidently influenced the establishment and development of the FHZ site, much remains unknown about how regional environmental changes specifically affected the use and eventual abandonment of cities. Furthermore, more precise chronological data is needed to directly link paleoenvironmental change with human activities during specific periods.

This study collected sedimentary information from various cores in different landforms of the FHZ site and conducted a comprehensive comparative analysis using geochemical element records, grain size parameters, and archaeological records. The objectives of this paper are to: (1) reconstruct the paleoclimate changes at the FHZ site, (2) analyze the evolution of regional landforms and hydrology in the study area, and (3) elucidate the relationship between climate fluctuations, hydrological dynamics, and the formation and decline of the FHZ site.

## Geographical setting

The study area is located in the southern part of the Nanyang Basin in the middle Yangtze River Valley, east of the HanJiang River (Fig. 1a). The Nanyang Basin is bounded in the southeast by the Dabie Mountains, in the southeast by the Jianghan Basin through the Suizhou Corridor, in the north by the Founiu Mountains, in the east by the Tongbai Mountains, in the west by the Qinling Mountains, and in the south by the remnants of the Daba Mountains. The edge of the basin is distributed with undulating granite, granite elevation of 140 ~ 200 m, granite interval with shallow and gentle river valley depression. The main rivers in the area are the Tang River, the Bai River, the Tujia River, the Dan River, and the Han River, which is the largest tributary of the Yangtze River (Fig. 1b). The study area has a northern subtropical monsoon climate. It is characterized by simultaneous rain and heat, and four distinct seasons. The main body of the study area is located in Xiangyang City, where the average annual temperature is between 15 ~ 16°C, except for the high mountains. The city is rich in heat resources and has a more obvious transitional nature, combining the characteristics of north and south climate. The city's annual precipitation ranges from 820 ~ 1,100 mm, of which 400 ~ 450 mm are recorded in summer. Solar radiation is relatively abundant, with an annual average total sunshine duration of 1800 ~ 2100 h. The Nanyang Basin is located in the central China, between the Yangtze River and the Yellow River, and is a hub between the north and the south [33].

The FHZ site (111°59'20.39"E, 32°14'042.67"N, highest elevation 94 m) is located in Xiangyang City, Hubei Province. The site is located in the eastern plain of the Hanshui River, open and flat in the north, and connected to the Dahong Mountain in the south, with the geomorphological features transitioning from alluvial plains and hilly plains to hills. fhz was built on an irregularly shaped terrace, and is bordered by the Paizi River in the east. The inner city of the site occupies an area of nearly 140,000 $m^2$, with a total area of about 500,000 $m^2$. The site is roughly square in plan, enclosed by walls and a moat. Centered on the FHZ site, a number of satellite sites were found in the surrounding area (Fig. 1b). Based on the total area of the FHZ site, the architectural remains within the city, especially the high-grade architectural sites, and the excavated jade and turquoise ornaments, it can be inferred that the site had a high status and was the regional center of Northwest Hubei [30].

## Materials and methods

# Stratigraphy and sampling

Combining the geomorphological and archaeological records, we chose the exploratory ditch excavated by Wuhan University at the site, which connects the southern city wall to the moat, for sample collection. The interior of the city walls contain house ruins, as well as extensive traces of braised red soil (Fig. 1d). The layers of the profile are clear, and several periods of falling water levels in between can be observed. The cultural layer is very thick, the internal accumulation of the moat can be divided into four periods: the historical period, the Meishan culture, the Shijiahe culture, and the Qujialing culture. It can be inferred from the pottery remains that the moat was used from the Qujialing Cultural period to the Ming and Qing dynasties. However, the use as well as the hydrological dynamics of each period varied greatly. The lithology of sediment cores was first observed in the field, and detailed lithological descriptions. The stratigraphic delineation is based on a combination of observations of soil color, texture, structure, and inclusions. The profile is described as Fig. 2.

# Chronology

The optical light (OSL) dating experiment was completed at the Shaanxi Key Laboratory of Earth Surface System and Environmental Carrying Capacity, NorthWest University, with a combined total of five samples. The experimental steps were as follows: (1) Prior to sample collection, the exposed portion of each sample was chipped in a laboratory darkroom to ensure accurate test results. Subsequently, the center portion of the sample was treated with a 30% solution of $H_2O_2$ and HCl to remove organic and carbonate material. (2) In order to obtain the quartz fractions required for dating, the medium-grained (45 ~ 63 μm) mixed minerals were screened using the wet sieve method. Subsequently, the feldspar component of the medium-grained mixed minerals was removed by using 30% fluorosilicic acid, resulting in a pure quartz sample for subsequent equivalent dose measurements. (3) Equivalent dose measurements were performed using a Risø-TL/OSL DA-15 DASH light release meter. During the measurements, the excitation light source was blue light (470 ± 30 nm) and the photomultiplier tube was preceded by two filters of U-340. The measuring instrument was equipped with a radioactive $\beta$-source $^{90}Sr/^{90}Y$ and all artificial radioactive irradiations were performed on this instrument. The monolithic regenerative dose (SAR) method was used to obtain accurate equivalent dose data. Detailed dating results are shown in Table 1.

AMS dating was conducted at Beta Analytic, USA. To mitigate the influence of organic contaminants, a standard acid-alkali-acid treatment along with solvent extraction was implemented before dating. The radiocarbon dates obtained in this study were calibrated using OxCal 4.3 and the IntCal13 calibration curve [34, 35] (Bronk, 2009, Reimer et al, 2013). Detailed dating results are shown in Table 2.

Table 1
OSL dating results from FHZ section.

| OSL No. | Depth (cm) | U (mg/kg) | Th (mg/kg) | K (%) | Dose rate-MAM (Gy/ka) | Dose rate-CAM (Gy/ka) | Aliquots (n) | MAM-De (Gy) | Age (a) |
|---|---|---|---|---|---|---|---|---|---|
| 01 | 55 ~ 85 | 1.98 ± 0.3 | 11.61 ± 0.7 | 1.82 ± 0.04 | 2.3 ± 0.31 | 2.65 ± 0.26 | 11 | 1.01 ± 0.09 | 788 ± 109 |
| 02 | 200 ~ 220 | 1.79 ± 0.3 | 10.38 ± 0.7 | 1.76 ± 0.04 | 4.38 ± 0.18 | 4.83 ± 0.28 | 20 | 2.48 ± 0.08 | 1611 ± 84 |
| 03 | 260 ~ 280 | 1.85 ± 0.3 | 11.25 ± 0.7 | 1.90 ± 0.04 | 5.32 ± 0.27 | 5.58 ± 0.16 | 32 | 10.51 ± 0.41 | 1837 ± 103 |
| 04 | 300 ~ 330 | 1.92 ± 0.3 | 11.28 ± 0.7 | 1.89 ± 0.04 | 5.74 ± 0.16 | 5.75 ± 0.12 | 23 | 21.28 ± 2.07 | 1985 ± 74 |
| 05 | 478 ~ 488 | 1.95 ± 0.3 | 12.15 ± 0.7 | 1.89 ± 0.04 | 17.67 ± 0.91 | 17.71 ± 0.46 | 19 | 19.73 ± 2.42 | 6042 ± 243 |

Table 2
AMS dating results from FHZ section.

| Laboratory No. | Depth (cm) | Cultural stage | $C^{14}$ Age (a) | Tree–ring dating(a)(95.4%) |
|---|---|---|---|---|
| Beta-597335 | 565 ~ 605 | Qujialing culture | 4430 ± 30 | 5060 ~ 4873 (67.7%) |
| Beta-597333 | 375 ~ 390 | Meishan culture | 3640 ± 30 | 4008 ~ 3868 (76.4%) |
| Beta-597334 | 505 ~ 530 | Meishan culture | 3740 ± 30 | 4165 ~ 3984 (90.5%) |

# Geochemistry

Geochemical elemental analysis experiments were completed in the Provincial Key Laboratory of Anhui Normal University as follows: (1)The samples were air-dried, and when the adsorbed water content was greater than 1%, the samples were dried in an oven at 50 ~ 60 ℃ for 24 h. The samples were then dried in an agate mortar and ground to less than 200 mesh, (2) Take more than 5 g of the dried samples and grind them in an agate mortar to less than 200 mesh, (3) Take the above grinding and mixing of powder samples 5 ~ 6 g into the plate mold with a diameter of 35 mm in a plastic cup, add 30 t pressure molding, pressing out the thickness of 2 ~ 4 mm disc. The discs were placed on an X-ray fluorescence spectrometer (XRF) for qualitative testing. The experimental instrument was a ZSX Primus IV X-ray fluorescence spectrometer

(XRF) produced by Rigaku, Japan. The analytical process was monitored by National Geochemical Standard Sediment Samples (GSS1 and GSD9), and the analytical error was less than ± 1%.

# Grain size

The particle size experiment was completed in the Marine Geology Teaching Laboratory of Nanjing University of Information Science and Technology. The experiment mainly includes two parts: sample pretreatment and instrumental measurement and analysis. The experimental steps are as follows: (1) Take 1 g of sample, add 10 ml of $H_2O_2$ solution and 10 mL of HCl solution in turn, and heat to remove organic matter and carbonic acid, (2) Add distilled water and leave it to stand, use a pipette to suck out the upper and middle clear liquid, (3) Add 10 ml of $(NaPO_3)_6$ solution with 0.5% concentration, and oscillate in an ultrasonic cleaner for about 10 min to obtain a highly dispersed suspension, (4) Measure the particle size with a laser particle size analyzer. The Mastersizer 2000 laser particle size analyzer was used to analyze 350 sediment particle size samples. The measurement range of the instrument is 0.02 ~ 2000 μm, and the relative error of repeated measurements is less than 2%. The particle size parameters mean particle size (Mz), sorting coefficient ($S_d$), skewness ($S_k$), and kurtosis (Ku) were calculated using the GRADISTAT program.

## Results

# Sediment chronology

Five OSL dates and three c14 samples were analyzed. One OSL sample (6024 ± 243 a) from 478 ~ 488 cm in the core is inverted and significantly older. Considering that it may have been affected by anthropogenic disturbance or lake erosion, it was not used to construct the chronological framework. After eliminating the outliers, the chronological depth model was constructed based on the Bayesian statistical method using the Bacon 2.2 program in R software [36]. The established chronological depth model is shown in Fig. 3:

# Characterization of geochemical elements

A comprehensive geochemical analysis of major oxides (MgO, $Al_2O_3$, CaO, $Na_2O$, $K_2O$) and trace elements (Rb, Sr, Ti) in the profile samples has been conducted, with the results detailed in Table 3. It also details the minimum, maximum, mean, standard deviation (SD) and coefficient of variation (CV) of the various elements at each stage and their comparison with the upper continental crust (UCC) [37]. The element distribution patterns and lithological variations in each stage provide crucial insights into the sedimentary environmental changes and hydrological dynamics recorded in the profile. Based on the distribution characteristics of these elements and changes in stratigraphic lithology, the profile has been divided into four stages (I, II, III, IV) for detailed discussion (Fig. 4):

Stage IV (625 ~ 550 cm, 5.5 ~ 4.5 ka BP): Compared with the UCC values, the contents of MgO(1.4%), $Al_2O_3$(13.8%) and CaO(1.2%) show significant depletion, and the CV is large, which indicating the different characteristics of the major elements during chemical weathering and deposition in the supergene

environment. The Ti content (4868.8 μg/g) was significantly enriched, with a decreasing trend from the bottom to the top. The mean value of Rb (126.9 μg/g) was higher than the UCC value and was also significantly enriched, while the mean value of Sr (103 μg/g) was lower than the UCC value and was significantly loss. The contents of Rb and Sr showed opposite trends, with the peaks of Rb corresponding to the troughs of Sr. Changes in geochemical element content fluctuate considerably in Stage IV, and it can be observed that such changes are associated with shifts in sedimentary environments.

Stage III (550 ~ 410 cm, 4.5 ~ 3.9 ka BP): The mean values of $Al_2O_3$(11.8%), CaO(1.6%), $Na_2O$(1%) show varying degrees of deficit compared to the UCC. The mean values of Rb(126.9 μg/g) and Ti(4119 μg/g) are higher than the UCC values and are enriched. the Sr(117 μg/g) shows a significant deficit. Overall, the variation of geochemical element content in stage III is relatively small, and the coefficient of variation is relatively small among the four stages. This indicates that the depositional environment was relatively stable at this time, and the source of materials was relatively single.

Stage II (410 ~ 210 cm, 3.9 ~ 1.6 ka BP): MgO(1.1%), $Al_2O_3$(11.2%), CaO(1.2%), $Na_2O$(1.1%) $K_2O$(2.2%) Sr(114.0 μg/g) showed a significant deficit compared to the UCC values, while Rb(114.5 μg/g), Ti(4481.9 μg/g) were enriched. Rb, CaO, MgO showed a gradual decreasing trend from bottom to top, while Ti and Na2O were the opposite. Among them, anomalously low values of Ti, Sr, $Na_2O$, $K_2O$, $Al_2O_3$, and MgO appeared in the interval of 280 ~ 220 cm (2.9 ~ 1.6 ka BP). This may be due to the occurrence of anomalous climatic events that affected the hydrological state at this time, resulting in the migration of geochemical elements. The trend of most of the geochemical element contents during this stage showed drastic fluctuations, which may be related to changes in the sedimentary environment and intensification of human activities, resulting in unstable migration or enrichment of the elements.

Stage I (210 ~ 0 cm, 1.6 ~ ka BP): After the anomalous deficit in Stage II, all the geochemical elements resumed a stable trend in Stage I. During 80 ~ 120 cm (0.8 ~ 1.1 ka BP), the contents of $K_2O$, MgO, and $Al_2O_3$ showed wave peaks and then began to decline again. However, in general, the magnitude of elemental changes became smaller and the coefficients of variation were low, which may be that the depositional environment changed back to a stable state.

Table 3
The content of major elements and trace elements in FHZ section at each stage.

| | | MgO(%) | $Al_2O_3$(%) | CaO(%) | $Na_2O$(%) | $K_2O$(%) | Rb(μg/g) | Sr(μg/g) | Ti(μg/g) |
|---|---|---|---|---|---|---|---|---|---|
| I | Min | 1.1 | 10.5 | 1.2 | 1.1 | 2.0 | 102.0 | 105.0 | 4449.0 |
| | Max | 1.3 | 12.8 | 1.4 | 1.3 | 2.2 | 114.0 | 119.0 | 4736.0 |
| | Mean | 1.2 | 11.5 | 1.3 | 1.2 | 2.1 | 108.8 | 113.5 | 4611.6 |
| | SD | 0.1 | 0.6 | 0.1 | 0.1 | 0.1 | 3.9 | 3.5 | 99.1 |
| | CV | 5.9% | 5.0% | 3.9% | 6.1% | 3.0% | 3.5% | 3.1% | 2.1% |
| II | Min | 0.9 | 8.7 | 1.1 | 0.8 | 1.8 | 102.0 | 87.0 | 3739.0 |
| | Max | 1.4 | 13.3 | 1.5 | 1.4 | 2.5 | 133.0 | 136.0 | 4788.0 |
| | Mean | 1.1 | 11.2 | 1.2 | 1.1 | 2.2 | 114.5 | 114.0 | 4481.9 |
| | SD | 0.1 | 1.1 | 0.1 | 0.2 | 0.2 | 7.8 | 11.6 | 293.1 |
| | CV | 11.3% | 10.3% | 7.5% | 13.4% | 8.9% | 6.8% | 10.2% | 6.5% |
| III | Min | 1.1 | 11.2 | 1.4 | 0.8 | 2.2 | 115.0 | 110.0 | 3956.0 |
| | Max | 1.4 | 12.3 | 1.7 | 1.1 | 2.4 | 124.0 | 125.0 | 4298.0 |
| | Mean | 1.2 | 11.8 | 1.6 | 1.0 | 2.3 | 119.2 | 117.0 | 4119.2 |
| | SD | 0.1 | 0.3 | 0.1 | 0.1 | 0.1 | 3.2 | 4.7 | 108.2 |
| | CV | 5.8% | 2.6% | 6.1% | 9.3% | 3.6% | 2.7% | 4.0% | 2.6% |
| IV | Min | 1.3 | 12.6 | 1.1 | 1.0 | 2.2 | 119.0 | 89.0 | 4478.0 |
| | Max | 1.5 | 14.4 | 1.3 | 1.2 | 2.5 | 134.0 | 119.0 | 5153.0 |
| | Mean | 1.4 | 13.8 | 1.2 | 1.1 | 2.4 | 126.9 | 103.0 | 4868.8 |
| | SD | 0.1 | 0.5 | 0.1 | 0.1 | 0.1 | 4.6 | 10.0 | 185.0 |
| | CV | 7.1% | 3.6% | 4.9% | 6.8% | 4.4% | 3.6% | 9.7% | 3.8% |
| | UCC | 2.5 | 15.4 | 3.6 | 3.27 | 2.8 | 84 | 320 | 3950 |

# Analysis of particle size parameters

Based on the Folk and Ward grain size classification criteria [38], the sediments in the profile section were categoriz Müller and Forstner ed into three grain size fractions: clay (< 4 μm), silt (4 ~ 63 μm) and sand (> 63 μm) In this study, several grain size parameter indices, such as median grain size ($M_d$), sorting ($S_0$), skewness ($S_K$), and kurtosis (KG), were used to reflect the grain size characteristics of the sediments. The results of the analysis of each particle size parameter are shown in Fig. 5, and the particle size variation of the whole profile can be divided into four stage:

Stage IV (625 ~ 550 cm, 5.5 ~ 4.5 ka BP): The raw soil layer (625 ~ 605 cm) consists mainly of silt (90.45%) and clay (8.52%). The $M_d$ content ranges from 6.19 ~ 6.56 μm, with minimal particle size variation. The $S_0$ ranges from 1.46 ~ 1.57, indicating poor sorting, and $S_K$ ranges from 0.19 ~ 0.3, suggesting coarse skewness. The KG ranges from 0.93 ~ 0.96, indicating medium KG. The stable $M_z$ suggests a consistent source, but the $S_0$ and KG values indicate physical effects such as water erosion during deposition. The upper layer (605 ~ 550 cm, 5.5 ~ 5.2 ka BP) is mainly silt (91.75%) and clay (7.61%), with sand content dropping to 0.63%. The $M_d$ ranges from 5.56 ~ 6.62 μm, indicating finer particles. The $S_0$ (1.39 ~ 1.53) shows poor sorting. $S_K$ (0.15 ~ 0.39) is mostly coarse (positive) and KG (0.89 ~ 1.15) is medium. These results suggest stable hydrodynamic conditions, typical of a lake or river environment.

Stage III (550 ~ 410 cm, 4.5 ~ 3.9 ka BP): This layer is primarily silt (89.36%) and clay (7.08%), with an increase in sand content (3.57%). The $M_d$ ranges from 5.57 ~ 6.59 μm. The $S_0$ ranges from 1.47 ~ 2.24 indicating poor sorting. The $S_K$ ranges from 0 to 0.38, mostly coarse (positive). The KG ranges from 0.89 to 1.43, indicating medium kurtosis. These granulometric results suggest strong and stable hydrodynamic conditions, likely a river environment.

Stage II (410 ~ 210 cm, 3.9 ~ 1.6 ka BP): This layer is mainly silt (90.15%) and clay (7.9%), with sand content further increasing to 1.96%. The $M_d$ ranges from 5.56 ~ 6.88 μm. The $S_0$ ranges from 1.44 ~ 2.63, indicating poor sorting. The $S_K$ ranges from − 0.17 ~ 0.39, mostly coarse (positive). The KG ranges from 0.89 ~ 1.63, indicating medium kurtosis. These results suggest a lake or river environment.

Stage I (210 ~ 0 cm, 1.6 ka BP ~ present): This layer is mainly silt (89.61%) and clay (8.93%), with sand content continuing to rise to 3.25%. The $M_d$ ranges from 5.47 ~ 6.39 μm. The $S_0$ ranges from 1.38 ~ 2.89, indicating poor sorting. The $S_K$ from − 0.23 ~ 0.42, mostly coarse (positive) and KG ranges from 0.95 to 1.52, indicating narrow kurtosis. These results suggest significantly increased hydrodynamic conditions. The $S_K$ supports this inference. The abnormal increase in sand content and poor sorting at 470 ~ 410 cm (4.0 ~ 3.9 ka BP) and 230 ~ 170 cm (1.7 ~ 1.4 ka BP) likely reflect local enhancements or changes in hydrodynamic conditions during deposition, possibly due to events like floods or storms.

## Discussion

# Holocene paleoclimate and sedimentary environment evolution

The sources, compositions, and content changes of geochemical elements in sediments are influenced by various factors, including watershed erosion, lake physicochemical processes, and the intrinsic geochemical behaviors of the elements during deposition [42]. Understanding these factors is fundamental for reconstructing past depositional environment changes. The Chemical Index of Alteration (CIA) is commonly used to reflect the degree of mineral alteration during weathering, an increase in CIA indicates enhanced chemical weathering. The determination of Be content is based on the degree of leaching of $Na_2O$ and CaO from the sediment relative to $Al_2O_3$, with lower values reflecting wetter depositional

environments. Saf is often used as an indicator of the degree of chemical weathering and climatic conditions of surface sediments and decreases with increasing weathering and warmth [42–44]. The Rb/Sr ratio reveals stratigraphic depositional environments and palaeo-climatic variations, and higher Rb/Sr ratios usually refer to warmer and wetter climates because Rb is relatively stable, while Sr is susceptible to loss in heavy precipitation conditions. Conversely, lower Rb/Sr ratios indicate arid climates. Mn/Ti values are lower in reducing environments because Ti is relatively stable in depositional environments, whereas Mn dissolves in reducing environments, thus indicating changes in precipitation [45]. Analysis of elemental ratios from the FHZ section reveals that CIA is negatively correlated with Saf and Be values, and positively correlated with Rb/Sr values (Fig. 6). Based on the elemental distribution characteristics and lithological changes, the paleoclimate changes at the FHZ site can be divided into four stages:

Stage IV (5.5 ~ 4.5 ka BP): The top of the raw soil layer is dated to about 5.2 ka BP, and it can be assumed that this moat was put into use during the early Qujialing culture (5.3 ~ 4.5 ka BP). Archaeological records show that the city wall was built during the Qujialing culture period. It shows that the moat and the wall should be built at the same time. The raw soil layer is dominated by silty clay, and the grain size characteristics indicate that this was originally a fluvial environment. The grains gradually became finer up to the upper layers, probably because it was after the construction of the moat tha the hydrodynamics weakened. The CIA, Rb/Sr, and Mn/Ti values were overall high, and the Saf and Be values were generally low. The combination of these data suggests that Stage IV was generally in a strongly weathered, warm and humid climatic environment. Among them, the values of CIA, Rb/Sr and Mn/Ti gradually increased during the period from 4.7 ~ 4.6 ka BP, reaching a peak at about 4.7 ka BP, while the Be values appeared to have a trough, confirming that the FHZ site was in a strong weathering, warm and humid climate at this time. Sporulation records from the Yangtze River Valley also show a significant increase in rainfall during this period (Fig. 6i). This also corresponds to the stage of stronger summer winds in East Asia recorded by the $\delta^{18}O$ sequence of Donggedong cave stalagmite DA (Fig. 6g). During 4.7 ~ 4.6 ka BP, the grain size parameters also showed abnormal fluctuations, which may be caused by heavy precipitation in warm and humid climates. The flood event carried a large amount of fine-grained material and deposited in the river channel, resulting in a decrease in the median particle size. Floods may bring sediments from different sources, making the $S_o$, $S_k$ and KG of sediments increase (Fig. 5). The content of medium-fine silt is prominent, and 10 ~ 40 μm accounts for a considerable share, which is consistent with the characteristics of multi-suspended silty sand in flood layer sediments [46]. During 5 ~ 4.5 ka BP, the climate of the Jianghan Plain was particularly unstable, and the lakes were in a period of instability or continuous change [47]. The two major flood events in the mid-late Qujialing culture (4.9 ~ 4.6 ka BP) and the late Shijiahe culture to the Xia Dynasty (4.1 ~ 3.8 ka BP) are common in the site strata of the Jianghan Plain [48]. However, from 4.7 ~ 4.5 ka BP, the CIA, Rb/Sr and Mn/Ti values gradually decreased to the valley value, and the Be and Saf values began to rise to the peak value. This indicates that the weathering is weakened and the climate gradually turns dry and cold.

Stage III (550 ~ 410 cm, 4.5 ~ 3.9 ka BP): 4.5 ~ 3.9 ka BP, CIA, Rb/Sr continued to remain low, and the Saf and Be trends were opposite. These indicators show a weakening of weathering, a decrease in rainfall, and a colder environment at this time. However, compared with stages II and I, the climate from 4.5 ~ 4.2 ka BP

was warmer. The stalagmite record shows that the East Asian summer winds weakened during this period compared to the previous period (Fig. 6g). The climatic drought events around 4.2 ka BP that occurred during this period spread throughout the northern hemisphere at low and mid-latitudes, and were an important cause of the decline of prehistoric civilizations and migration of peoples [49, 50]. Many large settlements in the Yangtze River basin, including the Shijiahe site, were abandoned [19]. The function of the city wall at the FHZ site disappeared, the moat continued to be used as a ring trench, and the site changed from a city site to a terrace-type ring trench settlement [30]. A severe flood event was recorded at the FHZ site stratigraphy around 4 ~ 3.9 ka BP. The CIA, Rb/Sr, and Mn/Ti were anomalously elevated, corresponding to peaks in Saf and Be values (Fig. 6). The $M_d$ of the sediments is anomalously elevated after a decrease, and the sand content is significantly higher (Fig. 6a; Fig. 6j). This is consistent with the stratigraphic record of flooding during the Qujingaling culture period mentioned above [48]. A major flood event caused by climatic fluctuations around 4000 a BP may have accelerated the collapse of the Shijiahe culture [51].

Stage II (410 ~ 210 cm, 3.9 ~ 1.6 ka BP): During the period of 3.9 ~ 2.7 ka BP, CIA, Rb/Sr generally show a decreasing trend, while Saf and Be values slightly increase. It indicates that weathering weakened and the climate continued to be dry and cool environment. Stalagmite records show a further weakening of monsoon action during this period (Fig. 6g). But the fluctuations in the elements indicate a very unstable climate at this time. At this time, the Meishan culture in northern China advanced southward to the Jianghan Plain to replace the Shijiahe culture, forming the Meishan culture Xiaojiayaoji type [52]. Until about 2.7 ka BP, the CIA, Rb/Sr started to rise, and the climate gradually changed to warm and humid. By 2 ~ 1.5 ka BP, the CIA, Rb/Sr rose sharply and peaked, while the contents of Saf and Be rose, but there was a trough. This shows that the depositional environment changed at this time, and it is speculated that this may be related to the southward migration of the Chu state [53]. In the 1.7 ~ 1.6 ka BP, were again abnormally elevated, and the$S_o$ and sand content were also elevated again. This indicates that at this time, the Fenghuangzui site was again subjected to flooding. This corresponds to the paleoflood layer (1597 a BP) of the DongJin Dynasty in the sedimentary record of the Jiangling profile in the Jianghan Plain [54].

Stage I (1.6 ka BP ~ present): The fluctuation of each environmental substitution index is pronounced. The overall environment of the Jianghan Plain exhibits a trend towards increasing aridity, characterized by intensified erosion, rapidly changing water levels, and shifting sedimentary conditions. These changes are significantly influenced by human activities. However, during the period from 0.8 ~ 0.2 ka BP, there is a notable decline in the CIA and the Rb/Sr ratio (Fig. 6b, Fig. 6d), alongside a marked increase in Saf and Be concentrations (Fig. 6e, Fig. 6f). This suggests a period of weak weathering and a cold, dry climate. Pollen records from this time also indicate a reduction in rainfall (Fig. 6i), which aligns roughly with the Little Ice Age during the Ming and Qing Dynasties (0.7 ~ 0.3 ka BP) [55]. Archaeological findings from ceramics further support this, indicating that the moat continued to be used during these dynasties.

# Multifactorial Considerations in the Site Selection for FHZ City

The site selection of prehistoric human settlements depended on two primary factors: efficient and convenient use of natural resources and avoidance of natural or social risks [56]. These factors were closely related to climate, regional hydrologic environments, and topographic and geomorphic contexts. Around 5.5 ka BP, the water levels of rivers and lakes in the middle Yangtze River decreased, expanding the land available for human settlement. This facilitated the increase and aggregation of settlements [57]. The fertile alluvial plains were suitable for rice agriculture, which eventually replaced hunting and gathering as the primary subsistence economy [19]. During the Qujialing-Shijiahe culture period (5.3 ~ 3.9 ka BP), early cities in the middle Yangtze River acted as regional centers controlling surrounding settlements, forming a four-tier settlement hierarchy: super city sites, large and medium-sized city sites, small city sites, and ordinary settlements [58]. The FHZ site, covering approximately 140,000 m², is classified as a large and medium-sized city site. To explore the relationship between the siting of the FHZ site and its regional hydrologic geomorphology, we used Geographic Information System (GIS) technology to assess the distribution of water systems and topographic contexts. By combining this data with records from other ancient city sites, we inferred potential reasons for early human selection of this site. The analysis results of the slope and orientation of prehistoric cities in the middle Yangtze River, the buffer zone, and the basin area are presented in Fig. 7 and Table 4:

Topographically, with the exception of the Longzui site, all of the early cities had slopes of 2° or less (Fig. 8a, Table 4), suggesting that gentle topography was an important site selection factor. This is because gentle terrain not only facilitates crop cultivation and irrigation, but also reduces the difficulties of farming caused by undulating terrain. In cities such as Shijiahe site and Yinxiang site, large areas of low-lying land were found, in which drilling and analysis revealed a high content of rice siliceous bodies [19, 59, 60]. These farming areas were 1 ~ 2m lower than the settlement areas, close to rivers and lakes, and connected to the water system [60]. Rice agriculture dominates the FHZ site, which has a slope of 0.4°, in line with the characteristics of the site selection of ancient cities in the middle Yangtze River. The results of aspect analysis show that there is no correlation between the orientations of the sites selected among the ancient cities, which may be related to the location of the water system around each of them(Fig. 8b, Table 4). The FHZ ancient city has a slope orientation of 198.4°, and its orientation belongs to the due south direction (159 ~ 203°). The moat of FHZ site flows eastward into a northwest-southeast oriented ancient river channel (called Qianwangxiaogou river), and then southeastward into the Paizihe River, a tributary of the Hanjiang River (Fig. 8). According to archaeological records, there are many remains of settlement sites and large areas of ancient floodplain deposits in the south of the city site (Fig. 8). The southern orientation of the inner city greatly enhanced accessibility to subsidiary settlements, facilitating communication and exchange. Considering the geomorphological characteristics of the river floodplain, it is likely that this area included cultivation zones, warranting further investigation.

Table 4
Analysis of topographical factors in prehistoric ancient cities in the middle Yangtze River

| No | Site | Slpoe(°) | Aspect(°) | Elevation(m) | Basin($km^2$) |
|---|---|---|---|---|---|
| 1 | Shijiahe | 0.4 | 281.3 | 31 | 1001 |
| 2 | Longzui | 2.1 | 202.2 | 32 | 1001 |
| 3 | Xiaocheng | 0.5 | 81.9 | 28 | 1001 |
| 4 | Taojiahu | 1.2 | 280.0 | 48 | 1001 |
| 5 | Menbanwan | 0.2 | 71.6 | 29 | 1001 |
| 6 | Yejiamiao | 0.4 | 90.0 | 29 | 1001 |
| 7 | Wangguliu | 0.6 | 104.0 | 63 | 1001 |
| 8 | Zhangxiwan | 0.4 | 31.0 | 30 | 1206 |
| 9 | Chenghe | 0.8 | 0.0 | 37 | 1720 |
| 10 | Majiawan | 1.0 | 8.1 | 59 | 1173 |
| 11 | Yinxiangcheng | 1.3 | 3.0 | 40 | 1173 |
| 12 | Jimingcheng | 0.6 | 14.0 | 39 | 1720 |
| 13 | Chengtoushan | 0.2 | 251.6 | 42 | 1725 |
| 14 | Jijiaocheng | 0.5 | 98.1 | 38 | 1725 |
| 15 | Qinghe | 0.7 | 71.6 | 36 | 1720 |
| 16 | Zoumaling | 1.0 | 118.3 | 32 | 1245 |
| 17 | Qixingdun | 1.6 | 285.3 | 55 | 1245 |
| 18 | FHZ | 0.4 | 198.4 | 88 | 932 |

The hydrologic analysis reveals that nearly all sites are within a 2 km buffer zone of the water system. A stable water supply from sources such as rivers, lakes, or springs was crucial for meeting domestic needs and supporting agricultural irrigation (Fig. 8c). Additionally, proximity to rivers facilitated waterborne transport and trade, thereby promoting economic growth [61]. Basin analysis, which delineates basins by identifying ridgelines, indicates that sites within the same basin are more accessible and connected. According to Table 4, basins measuring 1001 km² and below, as well as those 1720 km² and above, contain more ancient cities. These areas correspond to the regions south of the Dahong Mountains and the northwestern part of Dongting Lake, respectively, when considering modern water systems and landforms. The largest ancient cities in these regions are Shijiahe site (1200,000 $m^2$), and Chenghe site(600,000 $m^2$) [58]. These areas may have been key control zones for the Qujialing culture (Fig. 8c). The watershed containing the FHZ site borders that of the Shijiahe site, separated by the Dahong Mountain. As can be

seen from Fig. 7c and 8d, the western basin of Dahongshan corresponds to the Hanjiang River valley, which used to be controlled by the Majiawan and Yinxiangcheng sites. The eastern basin corresponds to the Suizao corridor, which used to be controlled by the Yejiamiao, Wangjialiu, and Zhangxiwan sites. This geographical distribution complicates efforts to protect the Shijiahe site. Without the watershed controlled by the FHZ site, northern cultures could have potentially invaded the Shijiahe site from both sides of Dahong Mountain. Consequently, in the event of an invasion by northern cultures, the FHZ site could relay warnings to the ancient city of Shijiahe via the Han River system. The Nanyang basin has historically served as a significant corridor for cultural exchange between northern and southern China [62]. The FHZ site played a pivotal role in facilitating the territorial expansion of the Qujialing-Shijiahe culture into the Nanyang Basin, situated at the confluence of the Jianghan Plain and the Central Plains. The establishment of the FHZ site served as a strategic outpost for the Qujialing culture in its interactions and conflicts with northern cultures.

The study area was selected for urban construction due to its proximity to water sources and agricultural suitability. The FHZ ancient city utilized the Qianwangxiaogou river to construct a moat, channeling water from the north to the Paizihe River. There are two ancient rivers about 20 meters wide in the city in a "T" shape. One runs east-west, passing east through the middle of the east wall and connecting with the moat (Fig. 8). This system introduced reservoir water into the city via moats, forming an irrigation network that ensured a stable water supply, supported rice agriculture and handicrafts, and served multiple functions such as transportation, defense, flood control, and drainage. Rice farming, the economic foundation of the region, offered high production efficiency, providing high-quality food and sustaining a large population [31]. Various sizes of rammed earth mounds were found in the city, primarily distributed along the east-west riverbanks and in other areas, where the main use would have been for flood control. The city site itself has an elevation of 88 m (Table 4), much higher than other sites. Around the wall length of about 170 ~ 280 m, width of 16 ~ 70 m, the overall higher than the outer lowland 1 ~ 2 meters. The choice of electing higher ground helped mitigate flood risks, and natural river bends slowed water flow, reducing flooding threats. The city was situated on elevated terrains such as hills, offering strategic vantage points and enhancing defense capabilities. The fertile soil between the rivers ensured agricultural productivity, securing food supplies. In addition, the site may have been chosen with transport connectivity and defence needs in mind. The dense river network ensures the efficient movement of people and goods, while creating natural topographical obstacles to minimize external threats.

# The Mechanism Driving the Rise and Decline of FHZ City

The sedimentary records from Miancheng core indicate that the most favorable climatic conditions in the Jianghan Plain occurred between 6.8 ~ 4.9 ka BP. From 6.8 ka BP onwards, there was evidence of river flooding, and numerous lakes were present across the Jianghan Plain during this period, which marked the precursor stage to the formation of Guyunmengze(Fig. 9b) [63]. From the Daxi culture to the Youziling culture (6.5 ~ 5.3 ka BP), ancient cities with walls, moats, and irrigation facilities, such as Chengtoushan and Longzi ancient cities, appeared in the Dongting Lake Basin and Jianghan Plain, benefiting from superior hydrological conditions [19]. The Youziling culture (5.7 ~ 5.3 ka BP) emerged on the left bank of the Hanshui River and rapidly spread westward, covering the area previously influenced by the Daxi culture.

During 5.3 ~ 4.5 ka BP, the study area experienced a warm and humid climate with increased weathering, providing favorable hydrothermal conditions for rice cultivation (Fig. 7). A large number of carbonized rice seeds from the Qujialing period were unearthed at the FHZ site [32].The Qujialing culture (5.3 ~ 4.5 ka BP), which developed from the Youziling culture, unified prehistoric cultures in the middle Yangtze River. This period saw significant societal transformations and a dramatic expansion of influence throughout the entire middle Yangtze River region. The Qujialing culture also exhibited a strong trend of expansion toward the central plains and maintained interactions with the Liangzhu culture in the lower Yangtze River region [64]. During this time, the weakening of the summer monsoon led to decreased rainfall, compelling ancient societies to develop irrigation systems to meet agricultural and domestic needs. This necessity likely promoted the emergence of ancient city sites and the development of complex social structures [19]. In addition, the frequent floods in the Jianghan Plain also prompted the Qujialing culture to build a perfect water conservancy system to withstand floods (Fig. 9a). Sections from the Zhongqiao site in the Jianghan Plain [65] and the Sanfangwan site within the Shijiahe site [48], as well as the Wuhan natural depositional borehole ZK145 [68], record flooding events that probably occurred during the middle of the Qujialing culture (Fig. 9a, Fig. 9b). Prehistoric ancient cities emerged in this period, such as Shijiahe city, Taojiahu city, Yinxiang city, Jimingchen city and other ancient city with walls and trenches, and appeared the embryonic form of central settlements and subordinate settlements [66]. The Shijiahe city became the central city of the middle Yangtze River, the social division of labor was refined, and there were large sacrificial places [58]. The walls at the FHZ site were constructed during the early Qujialing culture period (around 5.2 ka BP), likely reflecting a strategic need to expand northward. As the northernmost Qujialing cultural site, FHZ served as a critical gateway between the Jianghan Plain and northern regions. Archaeological evidence suggests that this area was the initial northern penetration point for the Qujialing culture from the Jianghan region, where it eventually established dominance. The culture later expanded into southeastern Shaanxi, southern and central Henan, and southwestern Shanxi [64]. The rise of the FHZ site is closely linked to the northward expansion of the Qujialing culture and frequent cultural interactions between the north and south. It was an important control point and possibly a military stronghold.

During 4.5 ~ 3.9 ka BP, the study area experienced a drier climate and further weakened weathering, but the early climate was still warm. The defensive function of the city wall at the FHZ site had disappeared, but the moat continued to serve as a ring trench, transforming the site from a city to a terrace-type ring trench settlement. Benefiting from the stable social environment and well-developed rice agriculture in the middle Yangtze River, the Qujialing culture was transformed into the Shijiahe culture and settlements gradually shifted from the terraces to the alluvial and lacustrine plains [62]. It is highly probable that the climatic changes sweeping across Eurasia between 4.2 ~ 4 ka BP led to the collapse of ancient civilizations, including that of the Yangtze and Mesopotamian Plains [19, 67]. Almost all major prehistoric cities in the Yangtze River basin were abandoned around 4 ka BP, with many settlements suddenly disappearing [62]. In addition, flood events were also a significant factor in the abandonment of the FHZ site. A major flood event that occurred at the end of the Shijia River has also been discovered at the Zhongqiao site and the Sanfangwan site [46, 65] (Fig. 9a). The flood event at the FHZ site in the Nanyang Basin corresponds roughly to the timing of the flood event recorded at the Jianghan Plain site as well as the Wuhan core [68]. However, the occurrence of flooding at the FHZ site was relatively short, which may be related to the high

topography. The shift in the function of the FHZ city during the Late Shijiahe culture period may have been due to the deposition of floodwaters that raised the moat and rendered the walls defenseless. The moat only had the function of irrigation left, and the FHZ city transformed into a weakly defended ring-trench settlement.

After the Shijiahe culture, the FHZ site was occupied by the Meishan culture from the Central Plains (3.9 ~ 3.7 ka BP) before being entirely abandoned. The Shijiahe culture is often associated with the Sanmiao cultural settlement, and the Sanmiao cultural settlement and the northern Central Plains cultural settlement often have large-scale conflicts and wars [69]. According to historical records, Yu, the leader of the Central Plains cultural settlement, attacked the Sanmiao cultural settlement when the middle reaches of the Yangtze River was hit by natural disasters such as heavy rains and earthquakes [47]. Evidence of cultural conflict has also been found in the Gujiapo cemetery near the FHZ site, with a large number of unearthed human bones and weapons showing the intensity of the war [70]. We hypothesize that after the walls of the FHZ site were rendered useless, the Xia culture in the north took advantage of the opportunity to invade. The Shijiahe ancient city, which is at a lower elevation than the FHZ site, was also caught in a flood disaster at this time, and the Xia culture was able to defeat the Sanmiao culture. The FHZ site lost its role as an outpost of the Shijiahe culture, so the Meishan culture was abandoned by the Xia culture at the transfer center afterward. At about 1.7 ~ 1.6 kaBP it was relatively dry, and with the discharge of the Dongjing River and Hanjiang River, the Jianghan Plain quickly dried up to land. At about 1.7 ka BP, the lake stabilizes and forms an alluvial plain (Fig. 9b) [63].

# Conclusions

This research reconstruct the geomorphological, hydrological, and climatic conditions of the regional environment surrounding the FHZ ancient city through detailed analysis of stratigraphic lithology, grain size parameters, and elemental geochemical records extracted from sedimentary sequences in the southern moat. These records provide a comprehensive reflection of climate variability, hydrological changes, and their implications for the cultural development history of the site during the mid-late Holocene.

(1) The stratigraphic profile of the FHZ ancient city provides a detailed record of environmental changes in the region since the mid-late Holocene. Between 5.5 ~ 4.5 ka BP, elevated CIA, Rb/Sr, and Mn/Ti values suggest a warm and humid climate conducive to intense weathering. A notable increase in grain size parameters around 4.7 ~ 4.6 ka BP indicates a flood event likely triggered by heavy rainfall. From 4.5 ~ 3.9 ka BP, declining CIA and Rb/Sr values alongside rising Saf and Be values indicate reduced weathering and a shift towards a cooler, drier climate. Another significant flood event occurred between 4 ~ 3.9 ka BP. During 3.9 ~ 2.7 ka BP, further declines in CIA and Rb/Sr values and slight increases in Saf and Be values suggest sustained dry and cool conditions with diminished weathering. Between 2.7 ~ 1.6 ka BP, rising CIA and Rb/Sr values indicate a transition to a warmer and more humid climate. Around 1.71.6 ka BP, another flood event occurred. From 1.6 ka BP to the present, climatic proxies show significant fluctuations. Notably, during 0.8 ~ 0.2 ka BP, sharp declines in CIA and Rb/Sr values alongside abnormal increases in Be and Saf values reflect the peak of the Little Ice Age during the Ming and Qing dynasties, marked by a significant temperature drop.

(2) The location of the FHZ city has a complex relationship with its geomorphology and hydrological environment. Early settlers strategically placed the walls on high ground and built moats to connect them to natural waterways. The river network is both a natural barrier and an important water source for rice cultivation. The design of the inner city, which faces directly south, takes into account the water system and agricultural areas. The purpose of Qujialing cultural settlement establishing FHZ city on the east bank of Han River is to expand its influence and protect the nearby Shijiahe city.

(3) The FHZ city was built in the early period of Qujialing culture (5.2 ka BP) to resist the northern culture and protect Shijiahe city. The warm and humid climate is conducive to agricultural activities, contributing to the prosperity of the city of FHZ. However, by the late Shijiahe culture (4 ~ 3.9 ka BP), the decrease of precipitation and temperature led to the decline of Shijiahe culture in the middle Yangtze River. Flooding events during this period rendered the FHZ walls defenseless. Subsequently, the FHZ city was invaded and eventually abandoned by the Meishan culture from the Central Plains. This refined analysis highlights the dynamic interplay between environmental factors and human settlement strategies in the FHZ ancient city, providing insights into its rise, adaptation, and eventual decline during the Holocene.

# Declarations


### Acknowledgements

Not applicable.


### Author contributions

Aipeng Guo: conceptualization, methodology, formal analysis, investigation, writing—original draft, writing—review and editing.

Longjiang Mao: investigation, resources, supervision, funding acquisition.

ChenChen Li: investigation.

Duowen Mo: validation, investigation, methodology, resources, supervision.


### Funding

This research was supported by Major Project of National Social Science Foundation of China: “Arrangement and Research on Archaeological Data of Zoumaling Prehistoric City Site”(19ZDA231).


### Availability of data and materials

The datasets used and/or analyzed during the current study are available from the corresponding author on reasonable request.

### Competing interests

The authors declare that they have no competing interests.

# References


1. Roberts N, Woodbridge J, Bevan A, Palmisano A, Shennan S, Asouti E. Human responses and non–responses to climatic variations during the last Glacial–Interglacial transition in the eastern Mediterranean. Q Sci Rev. 2018;184:47–67. https://doi.org/10.1016/j.quascirev.2017.09.011.
2. Panin A, Matlakhova E. Fluvial chronology in the East European Plain over the last 20 ka and its palaeohydrological implications. CATENA. 2015;130:46–61. https://doi.org/10.1016/j.catena.2014.08.016.
3. Xiao X, Zhao Y, Chi C, Zheng Z, Ma C, Liang C, Mao L, Hillman A. Quantitative pollen–based paleoclimate reconstructions for the past 18.5 ka in southwestern Yunnan Province, China. Glob Planet Change. 2023;230:104288. https://doi.org/10.1016/j.gloplacha.2023.104288.
4. Kumar V, Wang W, Zhang J, Wang Y, Ruan Q, Yu J, Wu X, Hu X, Wu X, Guo W, Wang B, Alipujiang N, Enguo L, Tang Z, Cao P, Liu F, Dai Q, Yang R, Feng X, Ping W, Zhang L, Zhang M, Hou W, Liu Y, Andrew B, Fu Q. Bronze and Iron Age population movements underlie Xinjiang population History. Science. 2022;376(6588):62–9. https://doi.org/10.1126/science.abk1534.
5. Xu D, Lu H, Chu G, Liu L, Shen C, Li F, Wang C, Wu N. Synchronous 500–year oscillations of monsoon climate and human activity in Northeast Asia. Nat Commun. 2019;10(1):1–10. https://doi.org/10.1038/s41467-019-12138–0.
6. Ardenghi N, Harning D, Raberg J, Holman B, Thordarson T, Geirsdóttir Á, Miller G, Sepúlveda J. A Holocene history of climate, fire, landscape evolution, and human activity in northeastern Iceland. Clim Past. 2024;20(4):1087–123. https://doi.org/10.5194/cp–20-1087-2024.
7. Blaus A, Nascimento M, Peterson L, McMichael C, Bush M. Climate, vegetation, and fire, during the last deglaciation in northwestern Amazonia. Q Sci Rev. 2024;332:108662. https://doi.org/10.1016/j.quascirev.2024.108662.
8. Fan D, Wu Y, Zhang Y, Burr G, Huo M, Li J. South flank of the Yangtze Delta: past, present, and future. Mar Geol. 2017;392:78–93. https://doi.org/10.1016/j.margeo.2017.08.015.
9. Méndez C, Nuevo–Delaunay A, Reyes O, Belmar C, Mena F. Early Holocene Archaeological Context and Assemblages of Baño Nuevo 1: A Key Site in Central West Patagonia. PaleoAmerica. 2024;1–18. https://doi.org/10.1080/20555563.2024.2327129.
10. Geirsdóttir Á, Miller G, Larsen D, Ólafsdóttir S. Abrupt Holocene climate transitions in the northern North Atlantic region recorded by synchronized lacustrine records in Iceland. Q Sci Rev. 2013;70:48–62. https://doi.org/10.1016/j.quascirev.2013.03.010.
11. Kaniewski D, Marriner N, Cheddadi R, Guiot J, Van C. The 4.2 ka BP event in the Levant. Clim Past. 2018;14(10):1529–42. https://doi.org/10.5194/cp–14-1529-2018.
12. Sun Q, Liu Y, Wünnemann B, Peng Y, Jiang X, Deng L, Chen J, Li M, Chen Z. Climate as a factor for Neolithic cultural collapses approximately 4000 years BP in China. Earth–Science Reviews. 2019;197:102915. https://doi.org/10.1016/j.earscirev.2019.102915.
13. Giosan L, Clift P, Macklin M, Fuller D, Constantinescu S, Durcan J, Stevens T, Duller G, Tabrez A, Gangal K, Adhikari R, Alizai A, Filip F, Vanlaningham S, Syvitski J. Fluvial landscapes of the Harappan

civilization, Proceedings of the National Academy of Sciences, 2012; 109(26), https://doi.org/10.1073/pnas.1112743109.

14. Huan X, Lu H, Jiang L, Zuo X, He K, Zhang J. Spatial and temporal pattern of rice domestication during the early Holocene in the lower Yangtze region China. Holocene. 2021;31(9):1366–75. https://doi.org/10.1177/09596836211019090.
15. Naudinot N, Kelly R. Climate change and archaeology. Quatern Int. 2017;428:1–2. https://doi.org/10.1016/j.quaint.2016.02.026.
16. Mousa F, El–Hassan M, Sallam E. Terminal Holocene palaeolake mud pans (playas) of Farafra Oasis, Western Desert, Egypt: palaeoenvironmental and palaeoclimatic implications. Int J Earth Sci. 2024;113(3):657–60. https://doi.org/10.1007/s00531-024-02395–w.
17. Ru T, Yang L, Wei G, Li X, Hou Z, Chen Y, Chen S. Mainstream migration events of the Yellow River and anthropogenic responses during the Mid–Holocene. Quatern Int. 2024;685:14–23. https://doi.org/10.1016/j.quaint.2024.01.010.
18. Du T, Zhang W, Li B, Liu L, Li Y, Ge Y, Yu S. Sedimentary evidence for the diversion of the Yellow River onto the North China Plain 3000–2600 years ago. Palaeogeogr Palaeoclimatol Palaeoecol. 2024;634:111909. https://doi.org/10.1016/j.palaeo.2023.111909.
19. Yasuda Y, Fujiki T, Nasu H, Kato M, Morita Y, Mori Y, Kanehara M, Toyama S, Yano A, Okuno M, Jiejun H, Ishihara S, Kitagawa H, Fukusawa H, Naruse T. Environmental archaeology at the Chengtoushan site, Hunan Province, China, and implications for environmental change and the rise and fall of the Yangtze River civilization. Quatern Int. 2004;123–5. https://doi.org/10.1016/j.quaint.2004.02.016.
20. Sun A, Zhao H, Ma M, Liu B, Li Y, Shi Z, Wang K, Li D, Xu Y, Chen F. Southward retreat of the Keriya River drove human migration in the Taklimakan Desert during the late Holocene. Q Sci Rev. 2024;332:108665. https://doi.org/10.1016/j.quascirev.2024.108665.
21. Wang C, Lu H, Zhang J, Gu Z, He K. Prehistoric demographic fluctuations in China inferred from radiocarbon data and their linkage with climate change over the past 50,000 years. Q Sci Rev. 2014;98:45–59. https://doi.org/10.1016/j.quascirev.2014.05.015.
22. Li B, Liu H, Wu L, et al. Linking the vicissitude of Neolithic cities with mid–Holocene environment and climate changes in the middle Yangtze River, China. Quatern Int. 2014;321:22–8. https://doi.org/10.1016/j.quaint.2013.11.018.
23. Liu J. Prehistoric Water Control Civilization in the Jianghan Plain. Beijing: China Social Sciences; 2023. (in Chinese).
24. Chen Dongfang. Development of moats and the origin of cities. Cult Relics Cent China, 2015(6): 42–5. (in Chinese).
25. Wu L, Li F, Zhu C, Li L, Li B. Holocene environmental change and archaeology, Yangtze River Valley, China: Review and prospects. Geosci Front. 2012;3(6):875–92. https://doi.org/10.1016/j.gsf.2012.02.006.
26. Li B, Zhu C, Wu L, et al. Relationship between environmental change and human activities in the period of the Shijiahe culture, Tanjialing site, Jianghan plain. China Quaternary Int. 2013;308:45–52. https://doi.org/10.1016/j.quaint.2013.05.041.

27. Li J, Wang S, Mo D. Environmental changes and relationship with human activities of Dongtinghu plain since 6000 a BP. Acta Scientiarum Naturalium Universitatis Pekinensis. 2011;47(6):1041–8. (in Chinese).
28. Xia Z, Kong X, Wang Y, et al. Accurating dating of D/O events during 95–56 ka BP in East Asian monsoon: A case study of stalagmites from Shanbao cave, Shennongjia, China. Scientia Sinica (Terrae). 2006;36(9):830–7. (in Chinese).
29. Deng H, Chen Y, Jia J, Mo D, Zhou K. Distribution patterns of the ancient cultural sites in the middle reaches of Yangtze River since 8500 a BP. Acta Geogr Sin. 2009;64(9):1113–25. (in Chinese).
30. Li Z, Wu T, Tian H. The Neolithic Site of Fenghuangzui. Xiangyang Hubei Popular Archaeol, 2021; (01): 12–5. (in Chinese).
31. Lou W. Analysis of starch granules from stone artifacts excavated from the Fenghuangzui site, Xiangyang, Hubei Province. Wuhan: Wuhan University; 2023. (in Chinese).
32. Huang X. Plant Macro-remains Unearthed from the 2020 Excavation at the Site of Fenghuangzui in Xiangyang. Wuhan: Wuhan University; 2023. (in Chinese).
33. Shi Z. Henan natural conditions and natural resources. Hena: Henan Science and Technology; 1983. (in Chinese).
34. Bronk RC. Bayesian Analysis of Radiocarbon Dates. Radiocarbon. 2009;51(1):337–60. https://doi.org/10.1017/s0033822200033865.
35. Reimer PJ, Bard E, Bayliss A, Beck JW, Blackwell PG, Ramsey CB, Buck CE, Cheng H, Edwards RL, Friedrich M, Grootes PM, Guilderson TP, Haflidason H, Hajdas I, Hatté C, Heaton TJ, Hoffmann DL, Hogg AG, Hughen KA, van der Plicht J. IntCal13 and Marine13 Radiocarbon Age Calibration Curves 0–50,000 Years cal BP. Radiocarbon. 2013;55(4):1869–87. https://doi.org/10.2458/azu_js_rc.55.16947.
36. Blaauw M, Christen JA. Flexible paleoclimate age–depth models using an autoregressive gamma process. Bayesian Anal. 2011;6(3):457–74. https://doi.org/10.1214/11-BA618.
37. Rudnick RL, Gao S. Composition of the Continental Crust. Treatise on Geochemistry. Elsevier; 2014. pp. 1–51. https://doi.org/10.1016/b978-0-08-095975-7.00301-6.
38. Folk RL, Ward WC. Brazos River bar: a study in the significance of grain size parameters. J Sediment Res. 1957;27(1):3–26. https://doi.org/10.1306/74d70646-2b21-11d7-8648000102c1865d.
39. Wang Y, Cheng H, Edwards RL, He Y, Kong X, An Z, Wu J, Kelly MJ, Dykoski CA, Li X. The Holocene Asian Monsoon: Links to Solar Changes and North Atlantic Climate. Science. 2005;308(5723):854–7. https://doi.org/10.1126/science.1106296.
40. Zhu C, Chen X, Zhang G, Ma C, Zhu Q, Li Z, Xu W. Spore-pollen-climate factor transfer function and paleoenvironment reconstruction in Dajiuhu, Shennongjia, Central China. Sci Bull. 2008;53(S1):42–9. https://doi.org/10.1007/s11434-008-5011-x.
41. Li J, Dodson J, Yan H, Wang W, Innes JB, Zong Y, Zhang X, Xu Q, Ni J, Lu F. Quantitative Holocene climatic reconstructions for the lower Yangtze region of China. Clim Dyn. 2018;50(3–4):1101–13. https://doi.org/10.1007/s00382-017-3664-3.

42. Perri F. Chemical weathering of crystalline rocks in contrasting climatic conditions using geochemical proxies: An overview. Palaeogeogr Palaeoclimatol Palaeoecol. 2020;556:109873. https://doi.org/10.1016/j.palaeo.2020.109873.
43. Wang P, Du Y, Yu W, Algeo TJ, Zhou Q, Xu Y, Qi L, Yuan L, Pan W. The chemical index of alteration (CIA) as a proxy for climate change during glacial-interglacial transitions in Earth history. Earth Sci Rev. 2020;201:103032. https://doi.org/10.1016/j.earscirev.2019.103032.
44. Chen C, Wang J, Wang Z, Peng Y, Chen X, Ma X, Cen Y, Zhao J, Zhou P. Variation of chemical index of alteration (CIA) in the Ediacaran Doushantuo Formation and its environmental implications. Precambrian Res. 2020;347:105829. https://doi.org/10.1016/j.precamres.2020.105829.
45. Chang H, An Z, Wu F, Jin Z, Liu W, Song Y. A Rb/Sr record of the weathering response to environmental changes in westerly winds across the Tarim Basin in the late Miocene to the early Pleistocene. Palaeogeogr Palaeoclimatol Palaeoecol. 2013;386:364–73. https://doi.org/10.1016/j.palaeo.2013.06.006.
46. Wu L, Zhu C, Li F, Ma C, Li L, Meng H, Liu H, Wang X, Tan Y, Song Y. Prehistoric flood events recorded at the Zhongqiao Neolithic Site in the Jianghan Plain, Central China. Acta Geogr Sin. 2015;70(7):1149–64. (in Chinese).
47. Shi C, Mo D, Liu H, Mao L. Late Neolcithic cultural evolution and environmental changes in the northern Jianghan Plain east of the Hanjiang River. Quaternary Sci. 2010;30(2):335–43. (in Chinese).
48. Wu L. Environmental Archaeological of the Mid–Holocene Palaeoflood in the Jianghan Plain Central China. Nanjing: Nanjing University; 2013. (in Chinese).
49. Kerr PJ, Tassier-Surine SA, Kilgore SM, Bettis EA, Dorale JA, Cramer BD. Timing, provenance, and implications of two MIS 3 advances of the Laurentide Ice Sheet into the Upper Mississippi River Basin, USA. Q Sci Rev. 2021;261:106926. https://doi.org/10.1016/j.quascirev.2021.106926.
50. Sionneau T, Bout-Roumazeilles V, Biscaye PE, Van Vliet-Lanoe B, Bory A. Clay mineral distributions in and around the Mississippi River watershed and Northern Gulf of Mexico: sources and transport patterns. Q Sci Rev. 2008;27(17–18):1740–51. https://doi.org/10.1016/j.quascirev.2008.07.001.
51. Guo L. Initial social complexity in the middle reaches of the Yangtze River (4300B, C, ~ 2000B, C). Shanghai: Shanghai Ancient Books Publishing House; 2005. (in Chinese).
52. Yuan F. Research on Meishan Culture, Wuhan: Wuhan University, 2020. (in Chinese).
53. Zhu C, Zhong Y, Zheng C, Ma C, Li L. Relationship of archaeological sites distribution and environment from the Paleolithic Age to the warring states time in Hubei Province. Acta Geogr Sin. 2007;62(3):227–42. (in Chinese).
54. Xie Y, Li C, Wang Q, Yin H. Sedimentary records of paleoflood events during the last 3000 years in Jianghan plain. Acta Geogr Sin. 2007; (01):81–4. (in Chinese).
55. Tao L, Su J, Kang Y. Reconstruction and analysis of chronology of high temperature events in eastern China during Ming and Qing dynasties. 2021; 23(02): 449–60. (in Chinese).
56. Li Z, Zhu C, Wu G, Zheng C, Zhang P. Spatial pattern and temporal trend of prehistoric human sites and its driving factors in Henan Province, Central China. Journal of Geographical Sciences, 2015; 25(9): 1109–1121. https://doi, org/10,1007/s11442-015-1222–7.

57. Zhao C, Mo D. Holocene hydro-environmental evolution and its impacts on human activities in Jianghan-Dongting Basin, middle reaches of the Yangtze River, China. Acta Geogr Sin. 2020;75(03):529–43. (in Chinese).
58. Liu H. The Settlement Structure and Social Form of Pre-Historic Cities in the Middle Reaches of the Yangzi River. Jianghan Archaeol, 2017; (05): 41–51. (in Chinese).
59. Nasu H, Momohara A, Yasuda Y, He J. The occurrence and identification of Setaria italica (L.) P. Beauv. (foxtail millet) grains from the Chengtoushan site (ca. 5800 cal B.P.) in central China, with reference to the domestication centre in Asia. Veg History Archaeobotany. 2006;16(6):481–94. https://doi.org/10.1007/s00334-006-0068-4.
60. Da H. The research on the relationship between culture and ecological environment of Neolithic Age in the middle reaches of Yangtze River. Hubei: Central China Normal University; 2009. (in Chinese).
61. Macklin MG, Lewin J. The rivers of civilization. Q Sci Rev. 2015;114:228–44. https://doi.org/10.1016/j.quascirev.2015.02.004.
62. Deng Z, Qin L, Gao Y, Weisskopf AR, Zhang C, Fuller DQ. From Early Domesticated Rice of the Middle Yangtze Basin to Millet, Rice and Wheat Agriculture: Archaeobotanical Macro-Remains from Baligang, Nanyang Basin, Central China (6700–500 BC). PLoS ONE. 2015;10(10):e0139885. https://doi.org/10.1371/journal.pone.0139885.
63. Zhu Y, Xue B, Yang X, Xia W, Wang S. Characteristic features of the sedimentary samples from the borehole M1 in Jianghan plain and reconstruction of paleoenvironment. J Geomech. 1997; (04):79–81. (in Chinese).
64. Shan S. A study on Qujialing culture, Wuhan: Wuhan University, 2019. (in Chinese).
65. Wu L, Zhu C, Ma C, Li F, Meng H, Liu H, Li L, Wang X, Sun W, Song Y. Mid–Holocene palaeoflood events recorded at the Zhongqiao Neolithic cultural site in the Jianghan Plain middle Yangtze River Valley, China. Q Sci Rev. 2017;173:145–60. https://doi.org/10.1016/j.quascirev.2017.08.018.
66. Wang H. The origin and function of moat settlement in the middle reaches of Yangtze River from the view of moat settlement in Menbanwan. Archaeology, 2003; (9): 61–75. (in Chinese).
67. Kajita H, Kawahata H, Wang K, Zheng H, Yang S, Ohkouchi N, Utsunomiya M, Zhou B, Zheng B. Extraordinary cold episodes during the mid–Holocene in the Yangtze delta: Interruption of the earliest rice cultivating civilization. Q Sci Rev. 2018;201:418–28. https://doi.org/10.1016/j.quascirev.2018.10.035.
68. Zhu H, Zhang Y, Li C. The application of end–member analysis in identification of paleo-floods in Wuhan section of the Yangtze River. Acta Sedimentol Sin. 2020;38(02):297–305. (in Chinese).
69. Liu B. Discussion on Sanmiao and Sanmiao Culture. Jianghan Archaeol, 2003; (04): 30–2. (in Chinese).
70. Jia H. On prehistoric intertribal conflicts in multi–culture areas in light of the excavation of the Gujiapo Cemetery. 2004; (04):77–86. (in Chinese).

# Figures

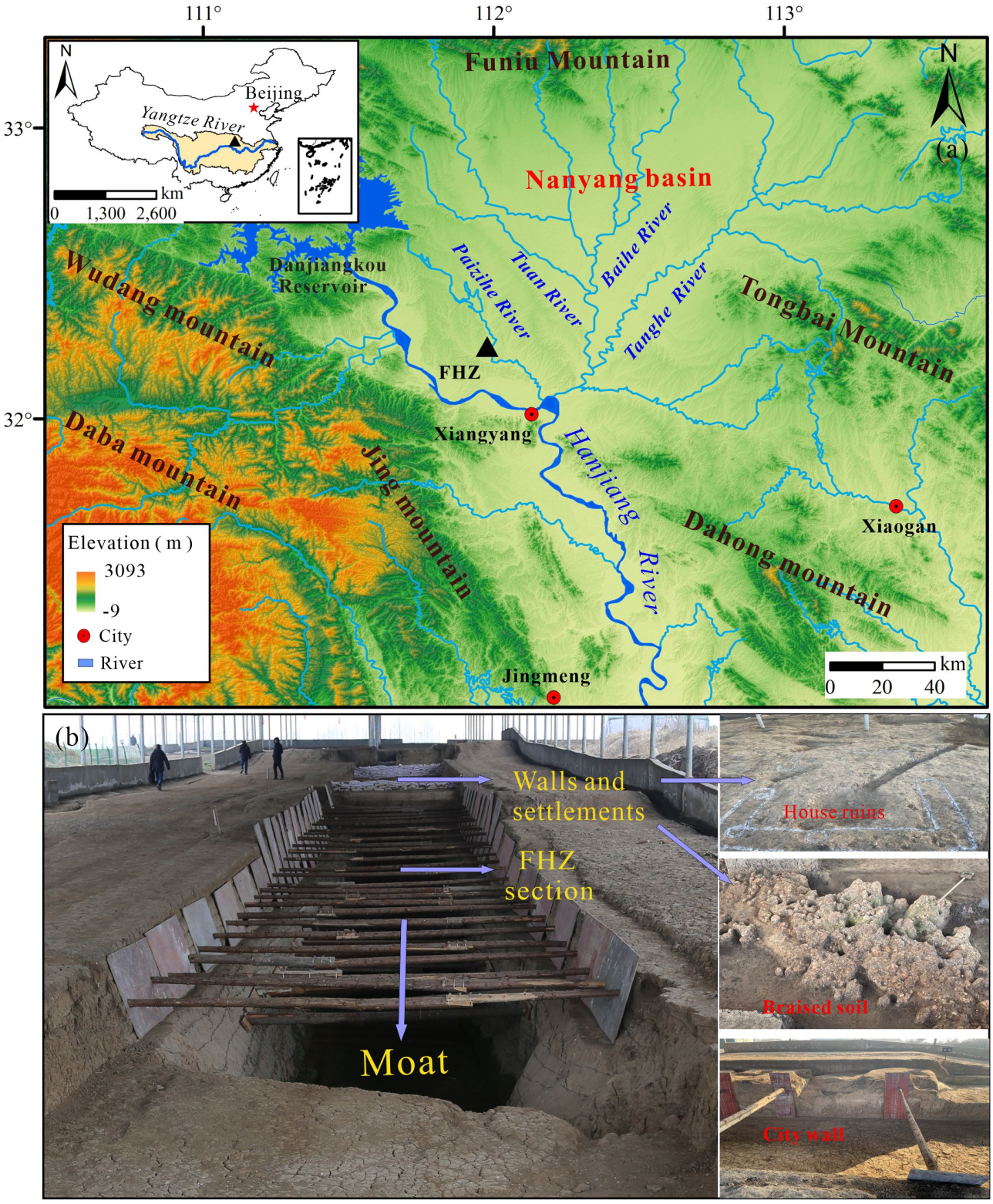


**Figure 1**

(**a**) Location of the study area in the Yangtze River Valley, (**b**) Sampling sites, the southern moat and archaeological remains.

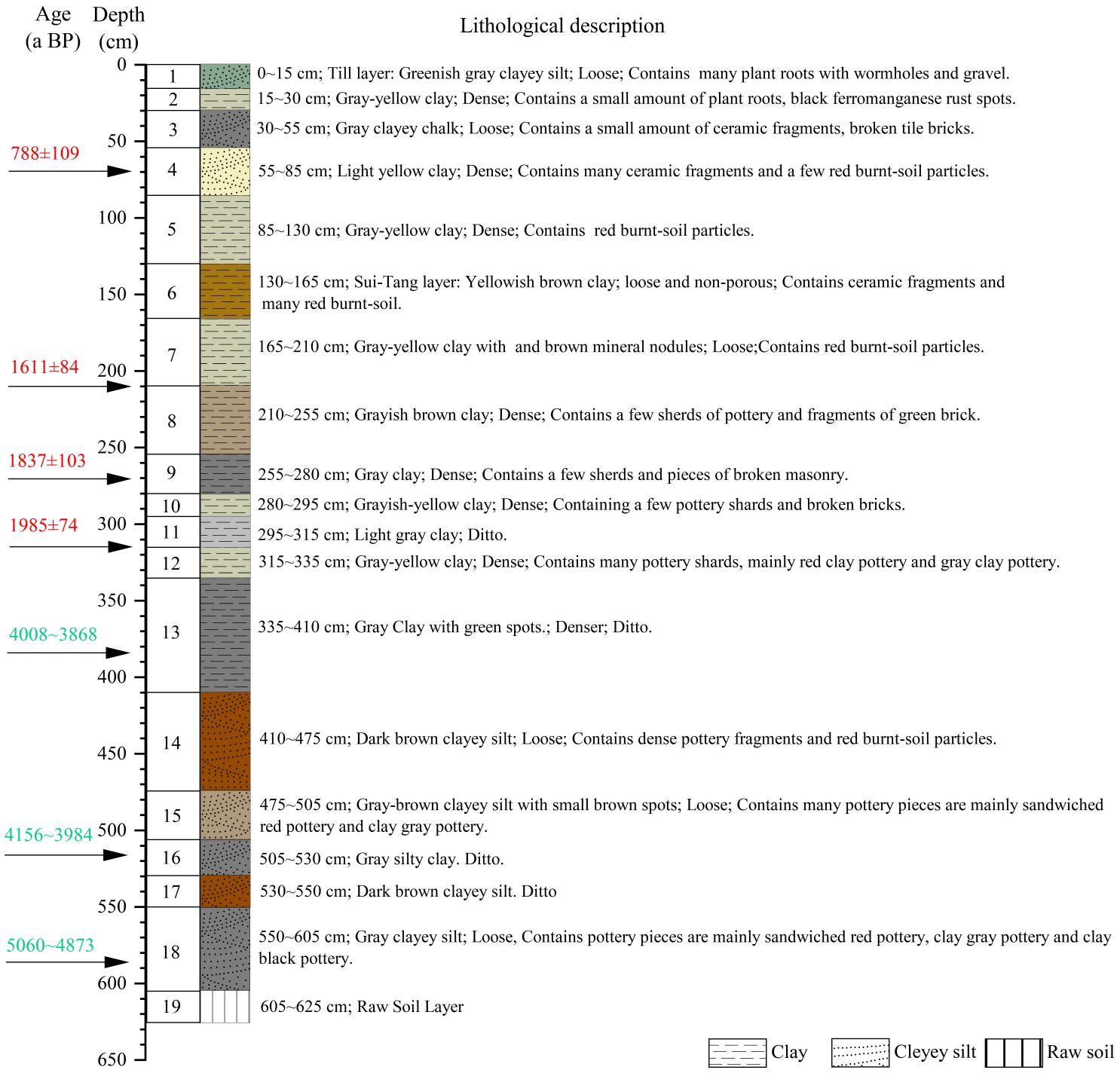


## Figure 2

Lithologic description and chronological sampling from the FHZ section (chronological red is photoluminescence samples, green is $C_{14}$ samples).

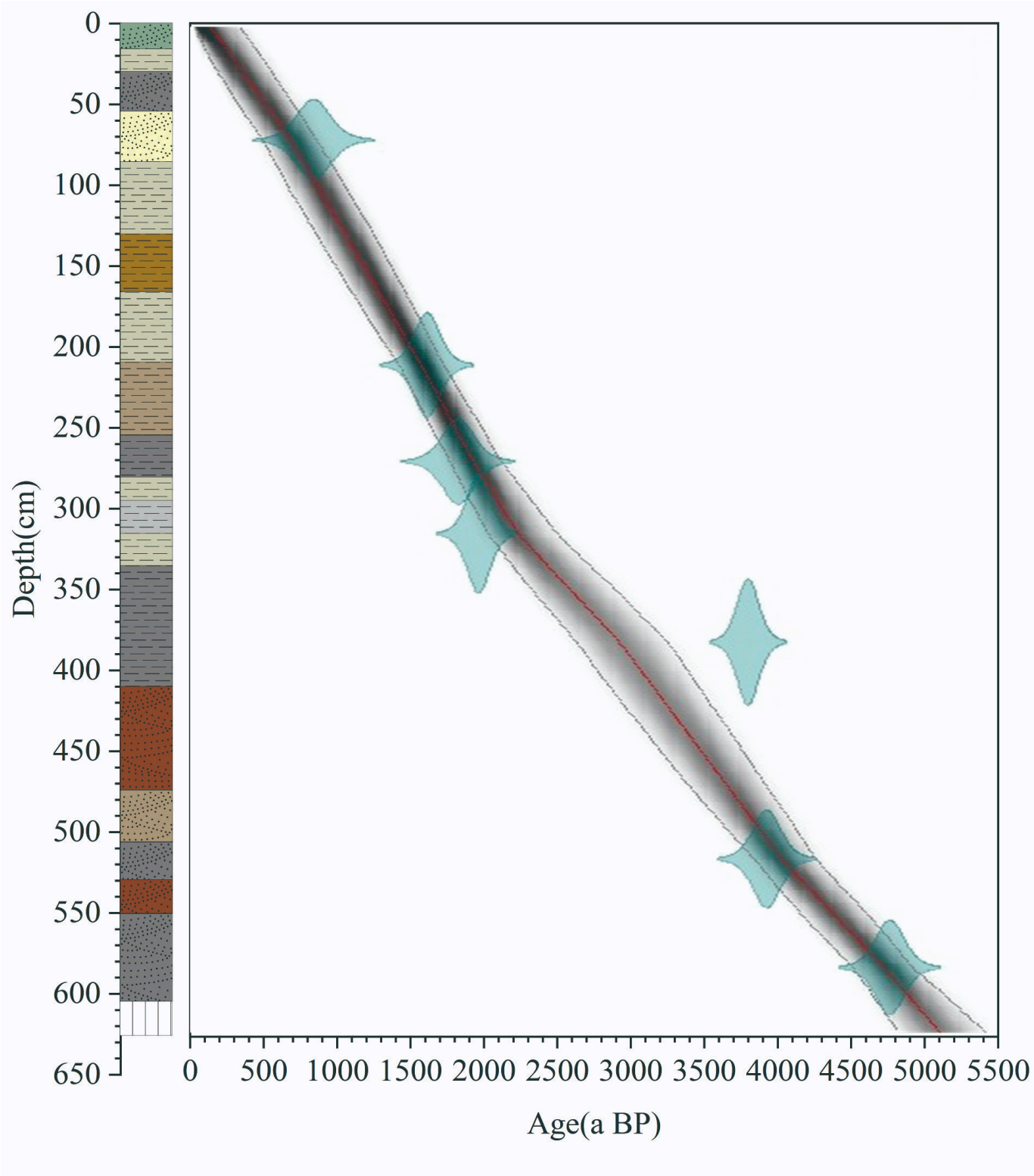


**Figure 3**

Age-depth model for FHZ section.

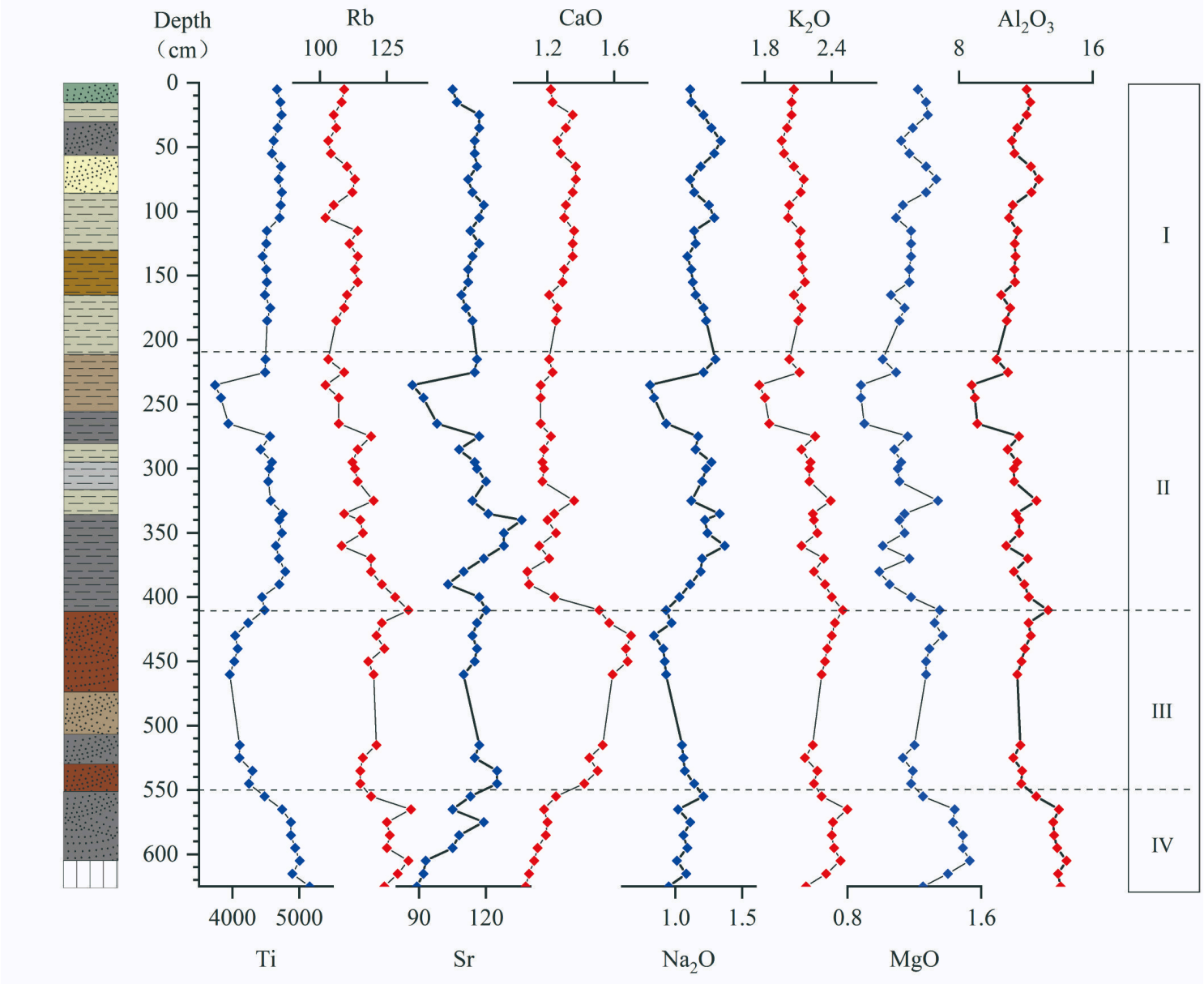


**Figure 4**

Vertical distribution of geochemical elements form FHZ section.

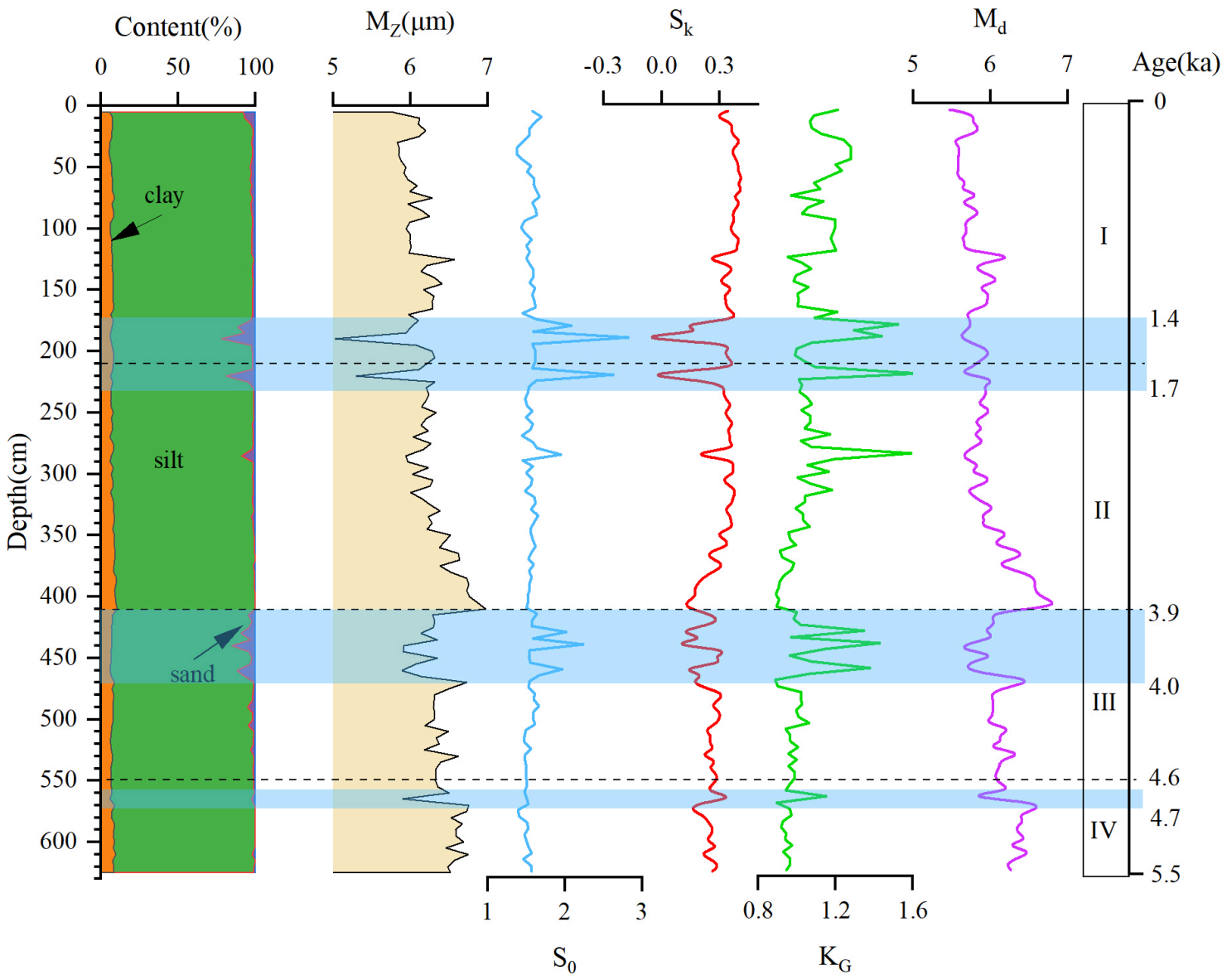


**Figure 5**

Vertical distribution of particle size parameters in FHZ profile.

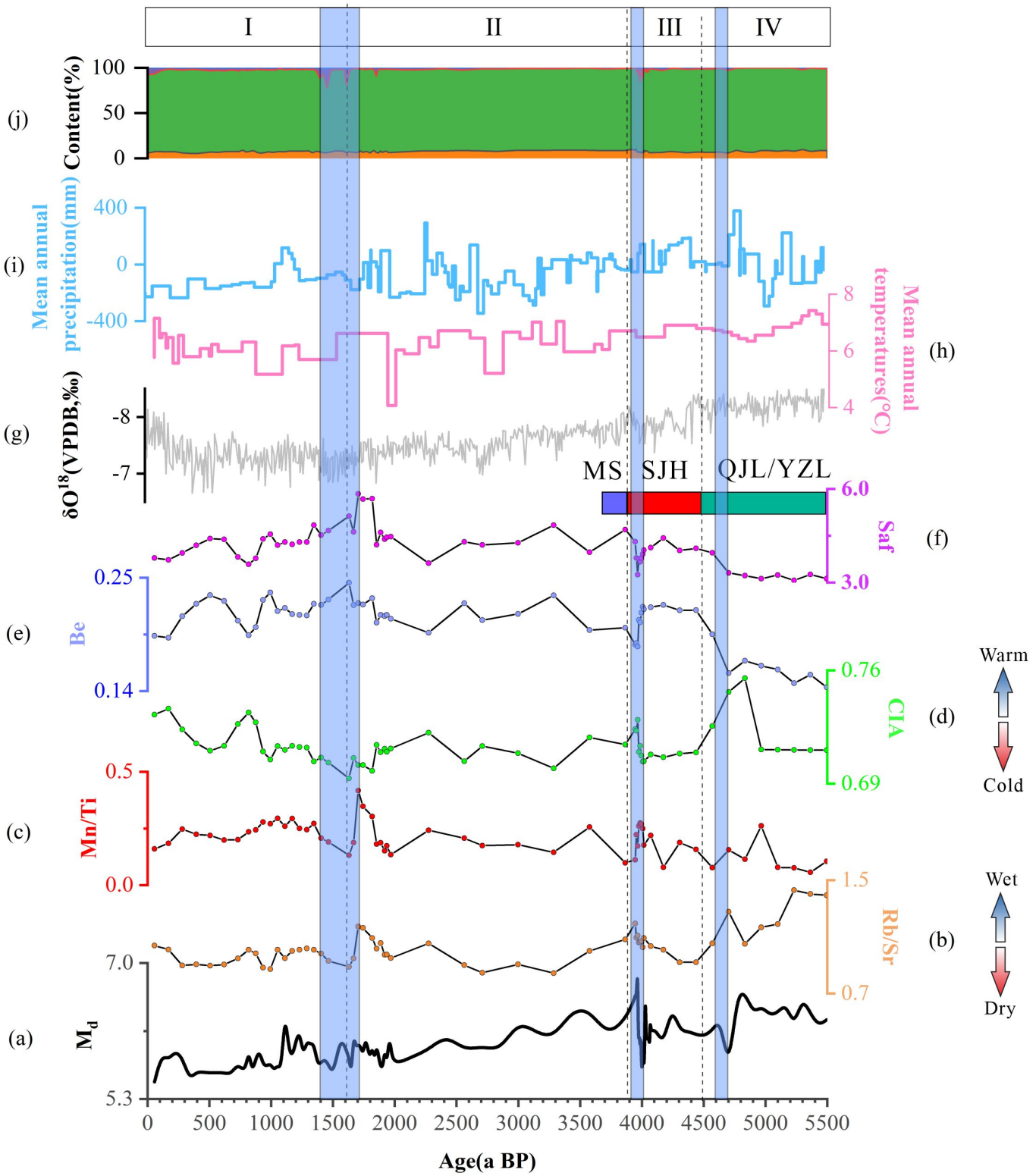


## Figure 6

Comparison of paleoclimate proxies form FHZ section: (**a**) Distribution of $M_d$ values form FHZ section. (**b**) ~ (**f**) Climate proxies of FHZ section. (**g**) $\delta^{18}O$ sequence of Dongge Cave stalagmite DA [39]. (**h**) Mean annual temperatures of pollen reconstruction from Dajiuhu Lake in the Shennongjia peat profile [40]. (**i**) Mean annual precipitation downstream of the Yangtze River based on pollen reconstruction [41]. (**j**) Grain size fractions form FHZ section. The QJL, SJH, MS and YZL in the color band represent the Qujialing

culture, the Shijiahe culture, the Meishan culture and the Youziling culture, respectively. The blue shaded area is the flooding period.

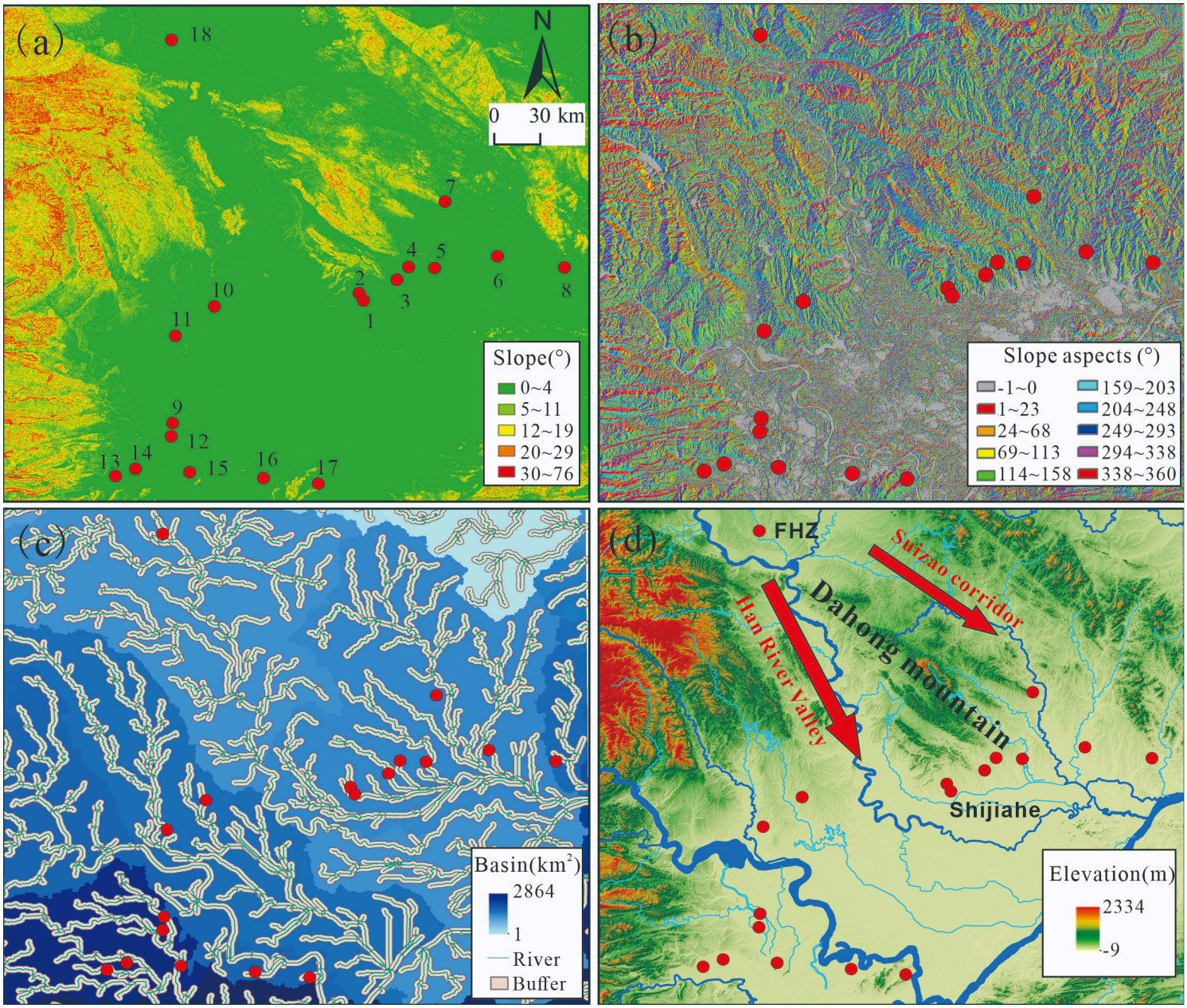


## Figure 7

(**a**)~(**b**) The distribution of slope and aspect of the ancient cities in the middle Yangtze River. (c) Analysis of river buffer zone (2 km) and basin. (d) Elevation extraction of ancient cities. (The prehistoric ancient city is 1: Shijiahe, 2: Longzui, 3: Xiaocheng, 4 Taojiahu, 5: Menpanwan, 6: Yejiamiao, 7: Wangguyao, 8: Zhangxiwan, 9: Chenghe, 10: Majiawan, 11 Yinxiangcheng, 12: Jimingcheng, 13: Chengtoushan, 14: Jijiaocheng, 15: Qinghe, 16: Zoumaling, 17: Qixingdun, 18: FHZ)

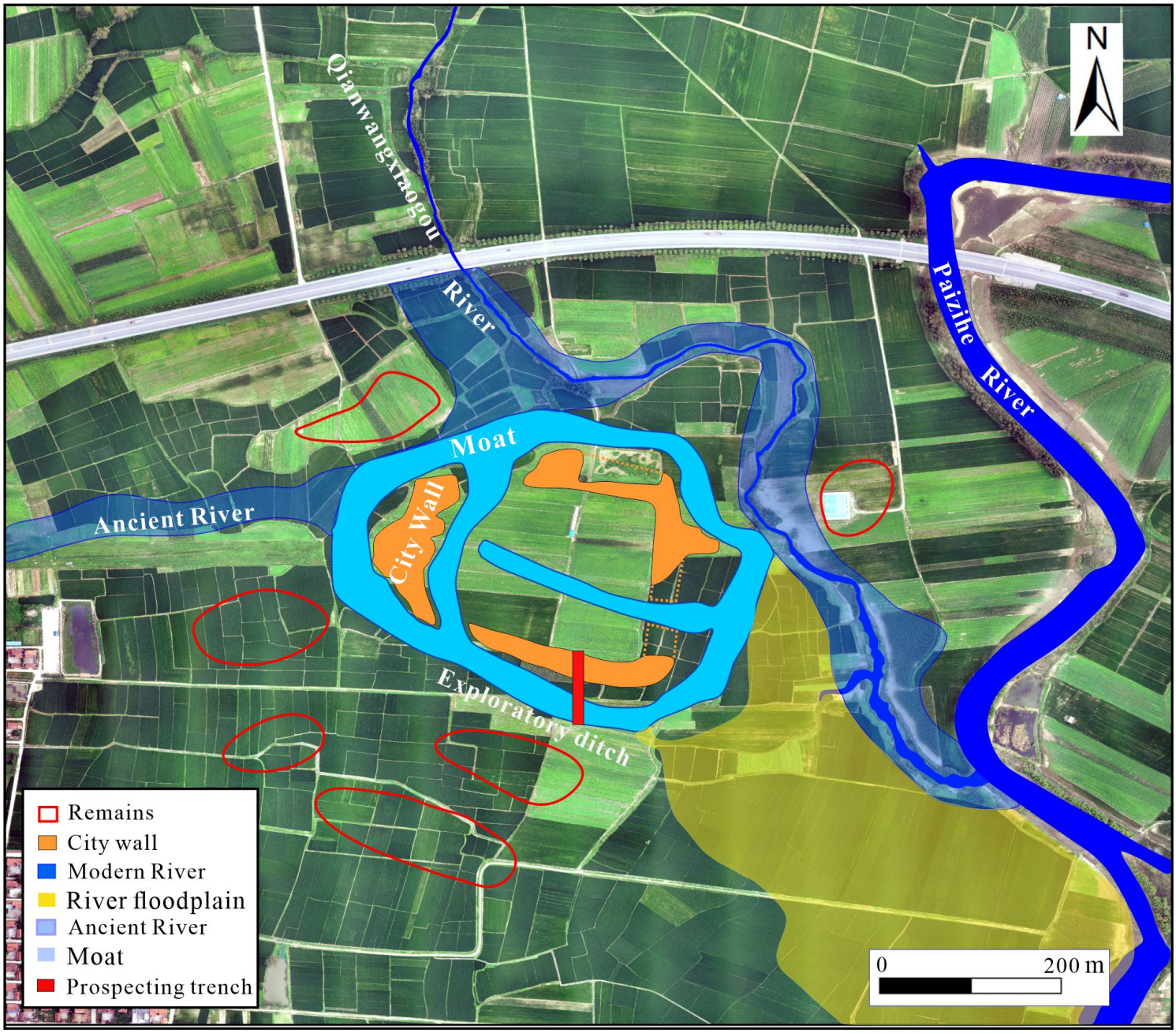


## Figure 8

Landscape schematic of the FHZ site.

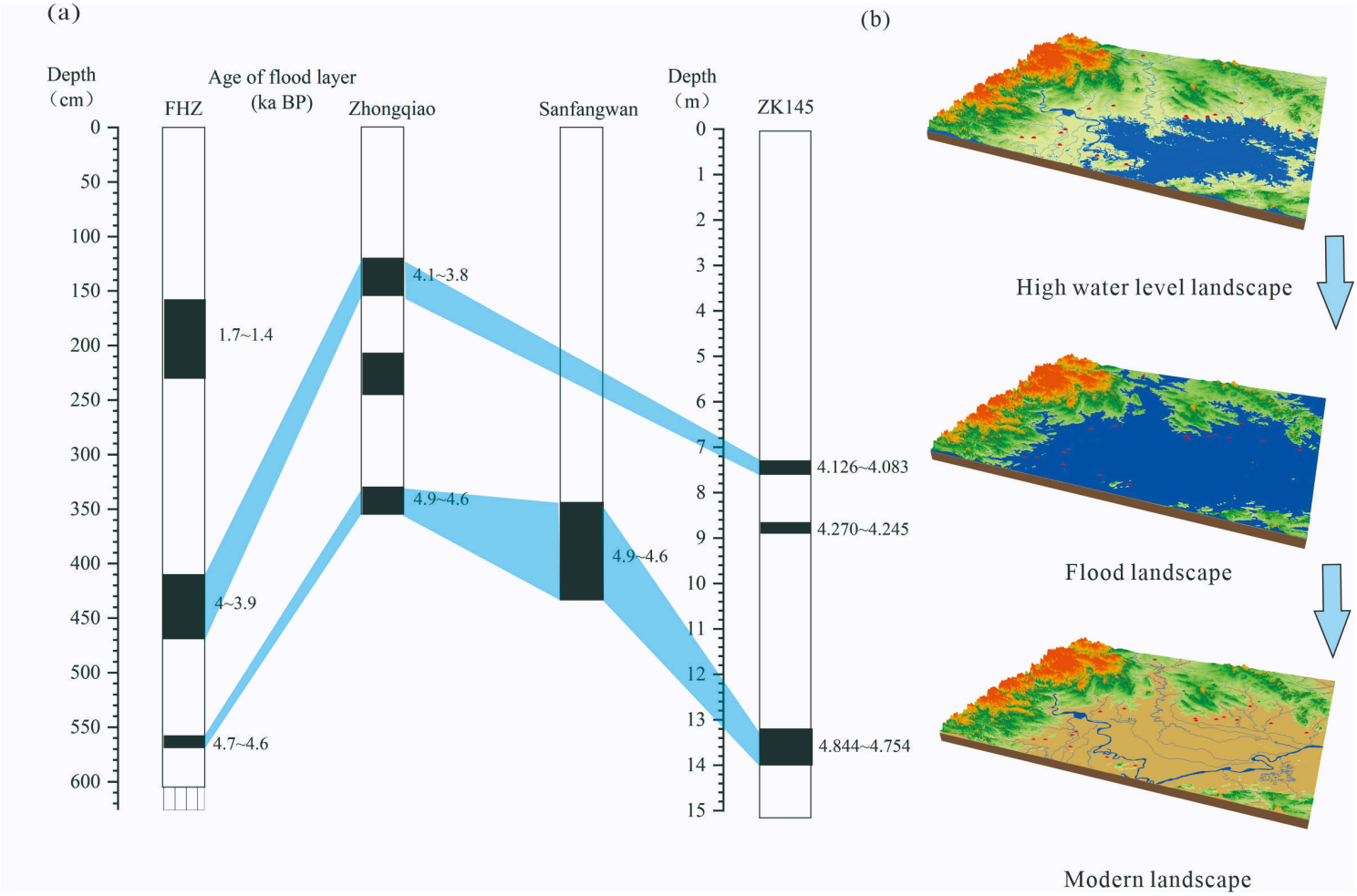


## Figure 9

(**a**) Comparison between the flood layer of the ruins in the middle Yangtze River [46, 65]and the borehole ZK145 in Wuhan [68]. (**b**) Landscape sketch map of the middle Yangtze River.